Mapping tropical forest degradation with deep learning and Planet NICFI data

Ricardo Dalagnol, Fabien H. Wagner, L. S. Galvão, Daniel Braga, Fiona M. Osborn, Le Bienfaiteur Takougoum Sagang, Polyanna C. da Conceição Bispo, Matthew Payne, Celso H.L. Silva Junior, Samuel Favrichon, et al.

Remote Sensing of Environment 298 (2023) 113798

Contents lists available at ScienceDirect

Remote Sensing of Environment

journal homepage: www.elsevier.com/locate/rse

Mapping tropical forest degradation with deep learning and Planet NICFI data

Ricardo Dalagnol [a,b,c,*], Fabien Hubert Wagner [a,b,c], Lênio Soares Galvão [d], Daniel Braga [d], Fiona Osborn [c], Le Bienfaiteur Sagang [a,c], Polyanna da Conceição Bispo [e], Matthew Payne [e,f], Celso Silva Junior [a,b,c], Samuel Favrichon [b,c], Vinicius Silgueiro [g], Liana O. Anderson [h], Luiz Eduardo Oliveira e Cruz de Aragão [d,i], Rasmus Fensholt [c,j], Martin Brandt [c,j], Philipe Ciais [c,k], Sassan Saatchi [a,b,c]

[a] Center for Tropical Research, Institute of the Environment and Sustainability, University of California, Los Angeles, Los Angeles, CA 90095, USA
[b] NASA-Jet Propulsion Laboratory, California Institute of Technology, Pasadena, CA 91109, USA
[c] CTrees, Pasadena, CA 91105, USA
[d] Earth Observation and Geoinformatics Division, National Institute for Space Research-INPE, São José dos Campos, SP 12227-010, Brazil.
[e] Department of Geography, School of Environment Education and Development, University of Manchester, Manchester, UK
[f] Institute for Environmental Futures, School of Geography, Geology and the Environment, University of Leicester, Leicester LE1 7RH, UK
[g] Instituto Centro de Vida (ICV), Alta Floresta, Mato Grosso, Brazil
[h] National Center for Monitoring and Early Warning of Natural Disasters - CEMADEN, São José dos Campos, SP, Brazil
[i] Geography, College of Life and Environmental Sciences, University of Exeter, Exeter EX4 4RJ, UK
[j] Department of Geosciences and Natural Resource Management, University of Copenhagen, Copenhagen, Denmark
[k] Laboratoire des Sciences du Climat et de l'Environnement, CEA-CNRS-UVSQ, CE Orme des Merisiers, Gif sur Yvette, France.

ARTICLE INFO

Edited by Marie Weiss

Keywords:
Forest degradation
Logging
Fire
U-net
Amazon

ABSTRACT

Tropical rainforests from the Brazilian Amazon are frequently degraded by logging, fire, edge effects and minor unpaved roads. However, mapping the extent of degradation remains challenging because of the lack of frequent high-spatial resolution satellite observations, occlusion of understory disturbances, quick recovery of leafy vegetation, and limitations of conventional reflectance-based remote sensing techniques. Here, we introduce a new approach to map forest degradation caused by logging, fire, and road construction based on deep learning (DL), henceforth called DL-DEGRAD, using very high spatial (4.77 m) and bi-annual to monthly temporal resolution of the Planet NICFI imagery. We applied DL-DEGRAD model over forests of the state of Mato Grosso in Brazil to map forest degradation with attributions from 2016 to 2021 at six-month intervals. A total of 73,744 images (256 × 256 pixels in size) were visually interpreted and manually labeled with three semantic classes (logging, fire, and roads) to train/validate a U-Net model. We predicted the three classes over the study area for all dates, producing accumulated degradation maps biannually. Estimates of accuracy and areas of degradation were performed using a probability design-based stratified random sampling approach ($n = 2678$ samples) and compared it with existing operational data products at the state level. DL-DEGRAD performed significantly better than all other data products in mapping logging activities (F_1-*score* = 68.9) and forest fire (F_1-*score* = 75.6) when compared with the Brazil's national maps (SIMEX, DETER, MapBiomas Fire) and global products (UMD-GFC, TMF, FireCCI, FireGFL, GABAM, MCD64). Pixel-based spatial comparison of degradation areas showed the highest agreement with DETER and SIMEX as Brazil official data products derived from visual interpretation of Landsat imagery. The U-Net model applied to NICFI data performed as closely to a trained human delineation of logged and burned forests, suggesting the methodology can readily scale up the mapping and monitoring of degraded forests at national to regional scales. Over the state of Mato Grosso, the combined effects of logging and fire are degrading the remaining intact forests at an average rate of 8443 km^2 year^{-1} from 2017 to 2021. In 2020, a record degradation area of 13,294 km^2 was estimated from DL-DEGRAD, which was two times the areas of deforestation.

* Corresponding author at: Center for Tropical Research, Institute of the Environment and Sustainability, University of California, Los Angeles, Los Angeles, CA 90095, USA
E-mail address: dalagnol@ucla.edu (R. Dalagnol).

https://doi.org/10.1016/j.rse.2023.113798
Received 19 January 2023; Received in revised form 16 August 2023; Accepted 30 August 2023
Available online 19 September 2023

1. Introduction

Degradation caused by selective logging and forest fires are the dominant forms of disturbance across tropical rainforests. It is responsible for up to 41.9% of total gross carbon emissions of the land use sector in the Amazon followed by deforestation (34.4%) and droughts (23.7%) (Aragão et al., 2014). Recent studies have shown that the Amazon Forest degradation has been increasing over the last decade, surpassing deforestation in affected areas and carbon losses up to three times (Matricardi et al., 2020; Bullock et al., 2020; Silva Junior et al., 2021; Qin et al., 2021). Unlike deforestation (total loss of forest through clear-cutting), the process of forest degradation causes partial losses of tree cover and carbon storage among other ecosystem services (Lapola et al., 2023). Degradation can be caused from direct management practices, such as selective logging and road construction, or from a series of hidden and collateral disturbances, such as understory fires, edge effects, forest fragmentation, and illegal logging (Asner et al., 2005; Souza et al., 2005; Pearson et al., 2017; Shimabukuro et al., 2015; Melendy et al., 2018; Shimabukuro et al., 2019; Silva et al., 2020). While fire is naturally suppressed in Amazon forests due to the humid understory microclimate (Uhl and Kauffman, 1990), it has become a widespread and increasing disturbance due to droughts. It can also have a synergistic effect with logging due to the opening of roads and clearings, which create dry surface fuel load and can exacerbate the risk and intensity of fires (Aragão et al., 2018; Barni et al., 2021; Silveira et al., 2022). The degraded forests, such as from logging activities, act as net carbon sources to the atmosphere, where the relative amount of carbon being emitted varies with intensity of disturbances (Mills et al., 2023). While degradation can lead to losses of carbon in tropical forests, sustainable practices in selective logging and/or the natural regeneration of these degraded forests post-disturbance can also lead to high rates of carbon accumulation if they are allowed to recover (Gourlet-Fleury et al., 2013; Bullock and Woodcock, 2021; Heinrich et al., 2023). Furthermore, degradation events across tropical rainforests remain largely undetected and underestimated from conventional remote sensing approaches, especially those related to selective logging, representing a major scientific gap on accurately estimating their impacts (Lapola et al., 2023).

Developing new methodologies for accurately quantifying forest degradation is essential for creating strategies to protect forests and their ecosystem services. These methodologies can be applied across various policy and action fronts, including the United Nations Framework Convention on Climate Change's (UNFCCC) Reducing Emissions from Deforestation and Forest Degradation (REDD+) program, which aims to monitor and reduce emissions from deforestation and forest degradation (Mitchell et al., 2017; Gao et al., 2020). In Brazil, new policies are being developed that involve payment for environmental services, which will require accurate data for forest monitoring (Brasil, 2021). Moreover, the recent increase in investments in forest carbon credits within the voluntary carbon market has also increased the demand for monitoring forests that are undergoing deforestation and degradation (Bomfim et al., 2022). Accurate monitoring is necessary to quantify emissions and attributions, to detect activity that are leaking into non-protected areas and causing emissions, and to monitor forests that are being preserved or restored (Joseph et al., 2013; Streck, 2021).

Accurate mapping of forest degradation in the tropics has been difficult to achieve due to the small scale of tree loss and the rapid recovery of tree canopies, which are significantly different from the large clear-cut disturbances caused by deforestation (Zhang et al., 2021; Aquino et al., 2022). For instance, treefall gaps created by selective logging are typically <25 m^2 and fully recover within two years (Dalagnol et al., 2019). Persistent cloud cover can also impede timely detection of these disturbances, as the spatial patterns of degradation may be obscured by the regrowth of understory vegetation before they can be observed in satellite imagery. Current initiatives are based on Landsat satellite data (30-m spatial resolution) in conjunction with machine learning methods and time series analysis to create global-scale maps of annual forest cover change that includes mostly clear cuts. Examples are the Global Forest Change (GFC) (Hansen et al., 2013) and the Tropical Moist Forests (TMF) (Vancutsem et al., 2021). The GFC product detects forest loss from clearing but also captures some levels of intense forest degradation (Cunningham et al., 2019; Kinnebrew et al., 2022). The TMF product includes separate information on degradation and deforestation, but it does not attribute or label the causes of degradation (Vancutsem et al., 2021). A newly derived product from GFC, called Global Forest Loss by Fire (here called FireGFL), disentangles the effects of forest fire and should be further tested over tropical regions (Tyukavina et al., 2022). The attribution of degradation is important because different degradation drivers, such as logging or fire, will lead to different carbon emissions from the disturbance which need to be estimated and accounted for (Rappaport et al., 2018). Also, national and global-scale burned area products with different spatial resolutions can also be used to assess forest degradation caused by fire. Examples are the MODIS MCD64 (Giglio et al., 2018), Fire CCI (Chuvieco et al., 2018), GABAM (Long et al., 2019), and MapBiomas Fire (Alencar et al., 2022). However, these burned area products may underestimate the occurrence of understory fires (Morton et al., 2011) and can have significant spatial dissimilarities, which indicates the uncertainty of these operational products (Pessôa et al., 2020).

Some disturbances related to forest degradation such as logging and fire have been traditionally mapped using spectral mixture analysis applied to medium spatial resolution data (e.g., Landsat satellites) to derive subpixel fractions that enhance the contrast between intact and degraded forests by logging and fire (Souza et al., 2005; Souza et al., 2013; Shimabukuro et al., 2019). By leveraging these fractions and conducting photo-interpretation, two operational forest degradation products have been created in Brazil: the Brazilian official deforestation and degradation alert program (DETER) for the Amazon forests (De Almeida et al., 2022), and the system for monitoring wood exploration (SIMEX) focusing on the Mato Grosso state (Silgueiro et al., 2021). These two products rely on the visual interpretation of images and manual editing of maps and require several months of work from a team of analysts to monitor one year of the area of interest. Subpixel fractions have also been used in other semi-automatic methods to map logging and fire in the Brazilian Amazon (Matricardi et al., 2010, 2020). However, Landsat data cannot directly observe disturbances and rely on changes in the reflectance signal (Dupuis et al., 2020; Gao et al., 2020), which can also be influenced by factors such as variability in rainfall, leaf density, or even acquisition artifacts. Additionally, high cloud cover in tropical regions limits the ability to detect all degraded areas, forcing some data products to have infrequent repeat time (3 to 4 years) (Matricardi et al., 2020). This reduces the ability to detect all degraded areas, whose effects may rapidly fade from the imagery (Dalagnol et al., 2019).

Norway's International Climate and Forest Initiative (NICFI) provides unprecedented open access to high-spatial resolution data (4.77 m) from Planet's satellite constellation for the entire tropics at bi-annual (twice a year) to monthly time scales (NICFI, 2021). A recent local-scale study exploring logging detection at multiple scales showed that the spatial resolution brought by PlanetScope data shows logging at low to medium intensity with success (Aquino et al., 2022). Another recent study explored the use of PlanetScope to map logging and fire-related degradation using traditional machine learning and texture metrics at local scale (Pinagé et al., 2023). Moreover, Planet NICFI mosaics aggregate data into a bi-annual scale from 2016 to 2020, and offer monthly mosaics from September 2020 until the present day through selecting the best cloud-free images. The high temporal resolution of the raw PlanetScope image acquisitions (close to daily) increases the chance of obtaining cloud-free data for the image composites generated, thereby increasing the possibility of mapping degradation in tropical forests. However, the usage of PlanetScope data does not come without limitations. For instance, the inter-calibration between the CubeSats

adds uncertainties in the data analysis of surface reflectance (Pandey et al., 2021). This makes it difficult to create robust large-scale applications because traditional machine learning and time-series algorithms operate on a per-pixel basis and largely depend on high-quality reflectance values. One potential solution is the application of DL methods for semantic segmentation, and more specifically, based on convolutional neural networks (CNN) (Lecun et al., 2015).

CNN methods are not constrained by specific values of a given pixel in the image, but they leverage the local textural variability as main sources of information to fit non-linear relationships at multiple levels of abstraction and map inputs into outputs with state-of-the-art accuracy (Lecun et al., 2015; Chollet et al., 2022). For example, they can identify two objects as cars in images because of common spatial features or patterns inherent to this type of target, despite having different colors. In the context of forest degradation, forest burn scars may show, for instance, different colors such as red and brown for recently burned areas, or light green for burned areas under vegetation regeneration. One can expect CNNs to be able to identify both areas as burn scars even though their spectral values (or colors, in terms of R, G, and B) may be totally different. Several CNN models are available such as U-Net, SegNet, FC-DenseNet or DeepLabv3+ among others (Ronneberger et al., 2015; Kattenborn et al., 2021). While the relative accuracy among these methods is similar for segmentation tasks, the U-Net has advantages such as simpler architecture, less effort for model training and inference, and low computational time (Lobo Torres et al., 2020). The U-Net has been widely applied with remote sensing imagery to find spatial patterns in high spatial resolution data, producing, for instance, maps of forest type and tree cover (Wagner et al., 2019; Brandt et al., 2020); tree species (Wagner et al., 2020; Dalagnol et al., 2022); roads (Botelho et al., 2022); and deforestation (Wagner et al., 2023). Because fire and logging disturbances create spatial patterns in the PlanetScope imagery that are observable to the human eye (e.g. trails, logging decks, and treefall gaps), it is expected that U-Net should be able to map them.

The Brazilian state of Mato Grosso is a major hotspot for forest degradation in the Amazon. From 2000 to 2013, 5890 km^2 of logging, 10,660 km^2 of forest fire, and 76,360 km^2 of deforestation were reported in Mato Grosso (Tyukavina et al., 2017). These numbers correspond to 43%, 52% and 32% of the whole Brazilian Amazon estimates, respectively. These estimates were based on the GFC data (Hansen et al., 2013) and represent a sample-based approach to disentangle the effects of each degradation type (Tyukavina et al., 2017). A spatially explicit map attributing the different degradation types to every unit of area has yet to be developed and validated and would be very valuable for REDD+ and forest monitoring operations. The state of Mato Grosso represents a highly relevant study area for testing a degradation mapping approach, due to the availability of regional datasets such as SIMEX and DETER that can be used to further evaluate the model predictions.

In this study, we develop and evaluate a methodology for mapping forest degradation with attributions in tropical rainforest ecosystems, using high spatial resolution satellite imagery from Planet NICFI and deep learning. We also introduce the DL-DEGRAD degradation product created by our methodology. Specifically, we present the process of training and validating a CNN U-Net model to map forest degradation with distinct attributions to logging, fire, and road construction, and evaluate the performance of the DL-DEGRAD by comparing it to available products. Our study addresses a major gap in forest monitoring and emission reduction programs and investments in avoiding deforestation and degradation, specifically the problem of accurately quantifying degradation - the second “D” in REDD+.

2. Materials and methods

2.1. Study area

The study area is the portion of the Amazon biome in the Brazilian state of Mato Grosso (Fig. 1). The area of 507,181 km^2 is mainly covered by open and dense ombrophilous forests and seasonal forests, as well as croplands and pastures. In the state of Mato Grosso, tropical forests have been threatened for decades by large-scale deforestation for commodity-driven agriculture and cattle grazing (Aragão et al., 2014). The slash-and-burn method used for deforestation, in conjunction with the use of fire as a land management practice, promotes the escape of fire to standing forests, causing understory fires. The development of new roads also drives the disturbance of forests (Ferrante and Fearnside, 2020; Nascimento et al., 2021). Moreover, Mato Grosso allows logging concessions in private lands for nominally sustainable wood extraction of non-threatened tree species. These concessions limit logging damage and extraction per hectare allowing the forest to regenerate over the next 25 years.

2.2. Forest degradation mapping methodology

2.2.1. Planet NICFI satellite data

We acquired bi-annual surface reflectance satellite data from the Planet NICFI product (‘analytic’ mosaic) having red (R), green (G), blue (B) and near-infrared (NIR) bands and a nominal spatial resolution of 4.77 m (NICFI, 2021). Each Planet NICFI quad (or tile) corresponds to 20 × 20 km in the ground and has 4096 × 4096 pixels. A total of 1530 tiles covered the study area (delimited by the red boundaries in Fig. 1) and were downloaded using scripts based on the PlanetNICFI R package v1.0.3 (Mouselimis, 2022). Data acquisitions encompassed the period from December 2015 to March 2022. This corresponded to 10 bi-annual Planet NICFI mosaics combining the best cloud-free images in a six-month window from January to June and from July to December of each calendar year from 2015 to 2020. The process of selecting the best cloud-free images is described in the NICFI documentation (NICFI, 2023). From 2020 we acquired 19 monthly mosaics (from September 2020 to March 2022), totalizing 29 image mosaics for the full period of analysis. The period of analysis covered 2016 to 2021, and the months of January, February and March of 2022 were used only for confirmation of detections in 2021. The NICFI product already filtered out some of the cloud cover from the mosaics. False positive degradation associated with the remaining clouds were removed in post-processing using a cloud mask applied to the derived maps, as described in a subsequent section (2.2.4). The only pre-processing step was a conversion from surface reflectance in integer (0 to 10,000) to 8-bit byte encoding (0 to 255) to compress the information to the number of levels necessary for the DL model. Since the reflectance of vegetation is low in the R, G, and B bands, we constrained their values up to a maximum of 2540 and scaled their distribution along the available 256 gray levels. Values above that threshold are usually found on very bright surfaces, such as clouds, and do not interfere with values from forest targets. NIR band values were not scaled because they already show a larger range of values than R, G, and B bands.

2.2.2. Degradation definition and sampling

In this study, forest degradation refers to forest-remaining-forest but being impacted by land use activities that modify properties of the stand or site and its carbon stocks resulting from a loss of canopy cover that is insufficient to be classified as deforestation (Pearson et al., 2017; IPCC, 2003). The definition may change depending on the forest definition in each country. For example, in Brazil, the forest is defined as land spanning >0.5 ha of trees with average height taller than 5 m, and >10% canopy cover. Degraded forest, therefore, refers to forests that after land use activities (e.g. logging, mining, edge effects, trails, roads, etc.) remain forest by definition. In our study, degradation refers to different intensity of logging and forest fires that partially remove forest canopy or burn understory trees, and logging trails and roads that may be temporary and narrow.

To train the model, we identified these areas using 4.77-m Planet NICFI satellite imagery (August 2021 mosaic) by observing spatial features such as canopy gaps, trails, logging decks, and specific color and

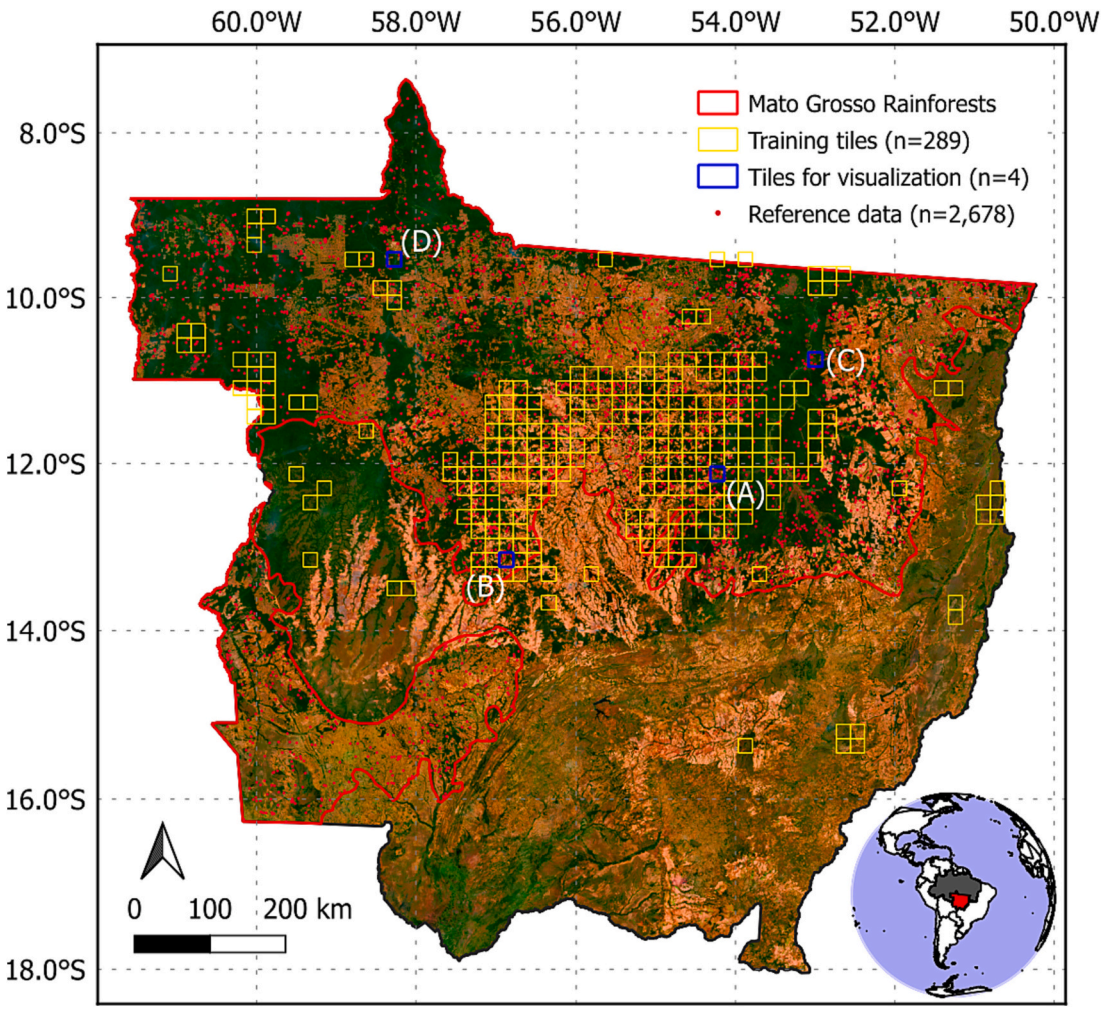

Fig. 1. Study area in the Brazilian state of Mato Grosso over the Amazon biome (red boundaries). The background consists of a Planet NICFI true color composite from August 2021, with overlaying training tiles in yellow (n = 289) and tiles used for visualization of results in blue (n = 4). Reference data used for design-based accuracy and area assessments were shown as red points (n = 2678). (For interpretation of the references to color in this figure legend, the reader is referred to the web version of this article.)

texture resulting from burning and recovery of forests (Table 1). This image composite was used because it had the best cloud-free observations. The mapping encompassed not only pixels with apparent tree loss and exposed bare soil, but also the surrounding context areas contouring these features observed in the imagery. This is based on evidence that logging can cause canopy damage to areas around logging trails and decks (Pereira et al., 2002; Asner et al., 2004), and that forest fires may cause direct but also delayed tree mortality from 5 to 10 years after fire, with long-lasting effects in terms of biomass up to 30 years (Silva et al., 2018). Therefore, we assumed as degraded those areas in between interleaved logging trails, in between and around multiple logging decks, and all forest areas within burn scars. These areas correspond to locations where trees have been effectively felled or burned, although the direct observation of tree loss or damage may be prevented due to occlusion caused by limited spatial resolution and multi-layer canopy (e.g. understory trees being felled or burned and not observed), or limited temporal resolution (e.g. vegetation quickly recovering of disturbance before the next image is acquired). This definition is in line with the current state-of-the-art of Brazilian degradation monitoring, based on visual interpretation of Landsat-like imagery, namely SIMEX (Silgueiro et al., 2021) for mapping both logging concessions and illegally logged forests, and DETER/INPE (De Almeida et al., 2022) the official dataset of forest degradation in the Brazilian Amazon, mapping both logged and burned forests.

We manually sampled a total of 289 tiles across the Mato Grosso state for a total of 115,600 km^2 sampled area. For each tile, all degradation occurrences were vectorized as polygons encompassing the whole degraded area and not only the individual spatial features of each disturbance type (e.g., isolated pixels of exposed ground at logged forests). Samples were collected and reviewed by three experts in degradation photo interpretation. From these tiles, we gridded the data into smaller image patches (256 × 256 pixels) and retrieved only those that intersected the presence of degradation in the manually delineated samples (n = 66,048 patches). To tackle heavy atmospheric effects identified in some bi-annual mosaics that were not present in August 2021 (e.g. dust-like cloud artifacts in Supplementary Fig. S1), we collected samples of the absence of degradation from the December-2016 and June-2017 bi-annual mosaics covering these areas (n = 7696 image patches of 256 × 256 pixels). The total sample size was 73,744 image patches.

The criteria used to sample logging included the presence of canopy gaps and/or multiple occurrences of logging decks and trails spread across a forest area. Logging decks and trails were regularly and irregularly organized across the landscape. Canopy gaps were not always observed on a logging site, likely due to small gap sizes, which can quickly close with vegetation regrowth (Dalagnol et al., 2019). The criteria used to sample fire included all burn scars observed in the landscape, including inside or outside forests, at different levels of

Table 1
Summary of degradation types, definition and image patterns used to detect disturbance visually in true color composites of Planet NICFI data.

Degradation type	Definition and image patterns visualized in the imagery
Logging	Boundary area around logging trails, decks, or treefall canopy gaps
a) Logging trail	Linear or curved features (e.g. 5–20 m wide). Sometimes called skid trails, these are temporary roads that are used for logging activities and to pull timber out of the forest. They may show exposed soil (white to magenta color) or regenerating vegetation (light green).
b) Logging deck	Small clearings (e.g. 15–30 m wide) with a rounded shape, where timber is temporarily stored before transportation. It may show exposed soil or regenerating vegetation.
c) Treefall canopy gaps	Small openings in the forest canopy with irregular shapes (e.g. 5–20 m wide) created by the tree felling process and with size varying according to logging damage. They reveal exposed ground or dead wood material (magenta), understory vegetation (light green), or shadows from neighboring trees (black), depending on the age and size of the gap and sensor view-illumination parameters. Gaps are not always directly observed in the imagery, but the texture of the recently logged canopy is rougher than that of the undisturbed forest.
Fire	Boundary area around burned forests or other land covers
a) Inside forests	Forest being brown- or grey-colored if the fire is recent; or a lighter shade of green if the fire is older and vegetation has been regenerating. Burn scars from large forest fires often show interleaving bands of burned forest due to different burning levels.
b) Outside forests	Exposed soil may show red, brown, or black colors due to the accumulation of burned coarse wood debris, ash, and charcoal. Areas with no forest remaining were filtered out of the final product.
Roads	Tree loss with linear or curved features (e.g. $\geq$ 20 m), consisting of unpaved roads or large trails surrounded by standing forest on both sides. It may show exposed soil or regenerating vegetation.

burned intensity and regeneration, and sometimes forests showing interleaved burning rings (Andela et al., 2022). The model was trained to recognize all burn scars, including inside and outside forests, and fires occurring outside of forests were then filtered out in post-processing to retrieve only standing forests degraded by fire. By including recent and older burn scars in vegetation, the model could learn patterns of forest fire at different levels of burn intensity and time since disturbance, possibly improving fire degradation detection even when new images were not readily available right after the fire event or with persistent cloud cover.

2.2.3. *U-Net model training*

To automatically segment forest areas affected by logging, fire, and road construction, we employed a U-Net model (Fig. 2) adapted from the original model from Ronneberger et al. (2015). The model has a u-shaped architecture due to the contracting path (encoder, left-hand side) that extracts contextual features at multiple spatial levels and a symmetric expanding path (the decoder, right-hand side) that localizes the features in the pixels to the size of the original image. On each level of the contracting path, there are two 3 × 3 convolutional layers followed by 25% dropout layers, a rectified linear unit (ReLU) activation function and a 2 × 2 max-pooling operation for downsampling. Meanwhile, in the expanding path, on every level there is a 2 × 2 upsampling of the feature maps from the lower level ("upconvolution"), concatenation with the feature maps from the matching contracting path, followed by two 3 × 3 convolutional layers and a ReLU. The final layer is a 1 × 1 convolutional layer with three outputs (logging, fire, and roads) with a sigmoid function, that is outputting a probability between 0 and 1 of a given pixel belonging to each class. The probabilities are then transformed into binary masks, converting values greater or equal to 0.5 to 1 (presence) and lower than 0.5 to 0 (absence), for logging, fire, and roads independently. We modified the original U-Net by changing the image input size to 256 × 256 pixels and by including four channels (R, G, B, and NIR), adding a new level of depth in the network (i.e., extra two convolutional layers at the beginning and end) and dropout layers in the contracting path with a value of 25%. The dropout layers help prevent overfitting of the model during the training phase by randomly setting to zero a portion of the output features (Chollet et al., 2022).

The model was trained using 80% of the samples, that is 58,995 image patches (256 × 256 pixels). To train the model, we used the Adam (adaptive moment estimation) optimization algorithm (Kingma and Ba, 2015) with a learning rate of 0.0001. The remaining parameters have been kept as default for *tensorflow* (beta_1 = 0.9, beta_2 = 0.999, epsilon = 1e-07, decay = 0). The loss function was calculated as the sum of

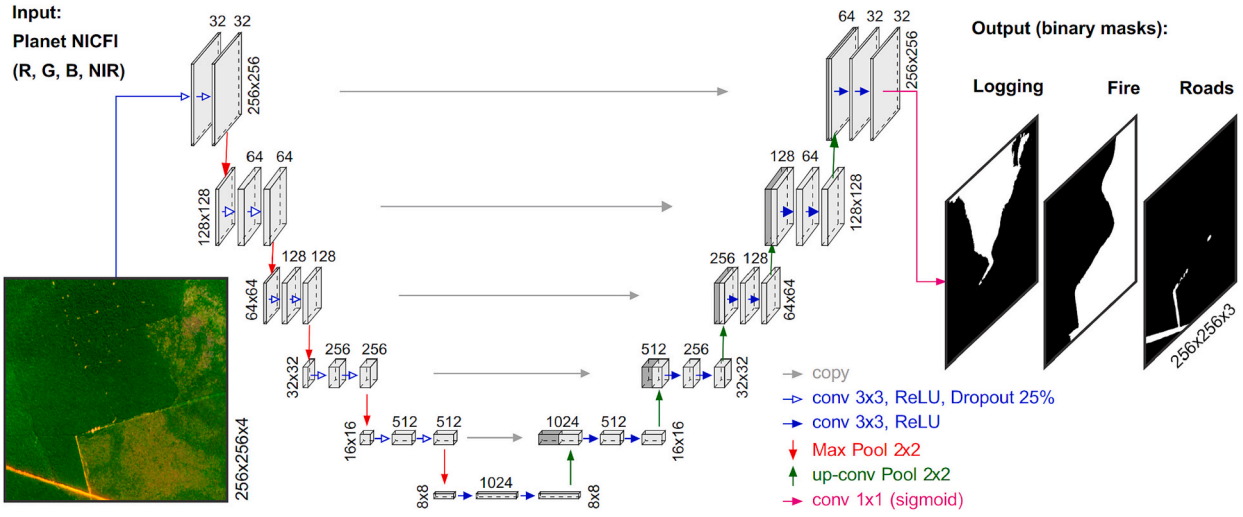

Fig. 2. The U-Net architecture used to map forest degradation. The model inputs the Planet NICFI Red, Green, Blue and NIR reflectance bands in image tiles of 256 × 256 pixels, which are processed through multiple convolutional layers. The final outputs include semantic segmentation (provided in binary masks) of logging, fire, and roads with the same pixel size as the input data. (For interpretation of the references to color in this figure legend, the reader is referred to the web version of this article.)

binary cross-entropy and Dice coefficient-related loss (Dice, 1945; Chollet, 2015; Allaire and Chollet, 2016). The network was trained for 1000 epochs with a batch size of 128 images and the model with the best *F_1-score* in validation was kept for prediction (epoch 900 with validation loss and *F_1-score* of 0.22 and 0.614, respectively; Supplementary Fig. S2). Data augmentation was randomly applied over the images during training to increase the samples' variability to improve learning (Chollet et al., 2022). The procedure included: (i) 0–360° rotations; (ii) horizontal and vertical flips; and (iii) ±20% changes to image brightness and contrast for all bands, and saturation and hue for the R-G-B bands, because the latter two augmentations work at the RGB color space. This step is important for the model to learn about shift invariance since degradation can happen in any orientation and shows high variability in reflectance. To run the DL model, we used *tensorflow* v2.6 through the *tensorflow* R package v2.9 (Falbel et al., 2022), and a RTX 3090 GPU with 24Gb memory.

2.2.4. Model prediction and post-processing

After training, the model was used to predict the three degradation types (Table 1) for all acquired Planet NICFI dates, creating binary masks (presence and absence) of each degradation type. Predictions were carried out for the entirety of Planet NICFI tiles for all 4096 × 4096 pixels at once. To avoid edge artifacts in the borders of the tiles, we added a border of 256 pixels to each side of the tiles. To create these borders, we used the data from the neighboring image tiles whenever available. Otherwise, we mirrored the borders from the same image (Ronneberger et al., 2015). Because the model was applied to predict over different landscapes than it was trained for, we visually inspected the predictions to identify areas with commission errors and added new samples over these areas. Also, given that the boundaries of degradation patterns are usually not sharp (e.g. forest and non-forest pixels), and thus subjective to be annotated by a human interpreter, we also re-evaluated how our training samples compared to the predictions and corrected labels that were incorrectly annotated or missed by the interpreters due to human error. These were included back in the training samples to improve the model iteratively.

Two post-processing procedures were applied to the bi-annual maps: (i) a bi-annual tree cover mask to remove detections outside the forest areas; and (ii) a cloud cover mask to filter out potential confusion due to cloud cover. The tree cover mask consisted of binary masks of forest/non-forest based on Planet NICFI data generated from a U-Net model with overall accuracy and an *F_1-score* above 98% validated with airborne LiDAR data, obtained from Wagner et al. (2023). The cloud cover mask consisted of binary masks of cloud/non-cloud based on Planet NICFI data and a U-Net model with the same architecture used in the study, showing 91.5% accuracy and 0.77 *F_1-score* on an independent test dataset. Cloud shadow was not considered for this filtering, because we did not identify degradation false positives associated with it. This complementary model and dataset were also developed and validated in this study and presented in Supplementary Material S1 as well as Supplementary Figs. S3-S5 for visual examples of the cloud cover mask results.

2.2.5. DL-DEGRAD product

The DL-DEGRAD product included three different layers (maps): bi-annual degradation, cumulative degradation, and detection frequency. The basic data output from the modelling approach consisted of binary degradation maps, which have a value of 1 for presence and 0 for absence of degradation, created for each disturbance type independently (logging, fire, and roads). For the period where we had monthly mosaics, we combined them into bi-annual degradation maps (months from January to June and from July to December) by taking the sum of all months within the 6-month periods, independently for each disturbance type. To reduce false positives in the dataset, we confirmed predictions from all bi-annual maps if (i) they had at least two detections in the 6-month window, or (ii) if they had one detection in the 6-month window, but also showed at least another detection within the three previous or next predictions, that is, a persistent signal. These confirmed pixels were set as value 1 (presence), and the remaining were set as value 0 (absence). This resulted in the bi-annual degradation maps for the time period from 2016 to 2021.

In the next step, we aggregated the bi-annual degradation maps into cumulative degradation maps from 2016 to 2021, where the value of each pixel was now set to the first image composite date of degradation occurrence in that pixel. In this map, 2016 represents all apparent disturbances visible in the imagery that year, while the remaining subsequent image composite dates represent new disturbances that have occurred over the areas. Therefore, the first year of the time series is not recommended for comparison with other forest degradation products. During this aggregation, the pixel values were simplified to 3-digits between 160 and 215 to encode the data in 8-bits and reduce file sizes. For example, 160 indicates the first half of 2016, while 165 indicates the second half of 2016, and so on until 215, representing the second half of 2021.

To generate the detection frequency map in the DL-DEGRAD product, we calculated how many times each pixel was detected for each type of degradation. A frequency greater than one does not directly mean the pixel experienced recurring disturbances, but indicates that the disturbance remains visible in the pixel over time. The frequency of detection allows further analysis of the degradation mapping to quantify the relative patterns of forest recovery, intensity of degradation, and the logging cycle.

2.3. Analysis

2.3.1. Model validation for individual mosaic prediction

To evaluate the performance of the model, we applied the trained model over 20% of the samples that were not used during training (14,749 image patches). The following four metrics were computed for quantifying the model performance, based on the pixel-by-pixel intersection per degradation type (Eqs. (1)–(4)):

$$\text{Accuracy} = (\text{TP} + \text{TN})/\text{NP} \tag{1}$$

$$\text{Precision}\ (P) = \text{TP}/\text{NPP} \tag{2}$$

$$\text{Recall}\ (R) = \text{TP}/\text{NPR} \tag{3}$$

$$\text{F1} - \text{score}\ (F_1) = (2 \times\ P \times\ R)/(P + R) \tag{4}$$

The true positive (TP) and true negative (TN) represent a match between prediction and sample data regarding the presence and absence of degradation, respectively. Accuracy represents the fraction of accurately mapped values in the map, considering both presence and absence of degradation. NP represents the total number of pixels, NPP represents the total number of presence pixels in the prediction, and NPR represents the total number of presence pixels in the reference. P represents the fraction of correctly mapped degradation, complementary to the commission error, while R represents the fraction of reference data accurately mapped by the model, complementary to the omission error. Finally, F_1 represents the harmonic mean between P and R, that is, a balance between commission and omission errors.

2.3.2. Estimating accuracy and area

To provide estimates of accuracies and areas for DL-DEGRAD results as well as inter-compare data products, we followed the good practices considering a design-based stratified random sampling approach (Olofsson et al., 2014; Olofsson, 2021). We distributed a total of 2678 samples across the region for our analyses (Fig. 1). The DL-DEGRAD maps were used to stratify the landscape into presence and absence strata of degradation classes. Since the majority of land cover in this region is nominally undisturbed forests or non-forest, and degraded forests are a rare class in this region (< 7% cover each type), we selected

a minimum of 300 samples for each disturbance type from the maps to be distributed randomly across any year of disturbance between 2017 and 2021. The remainder of samples were randomly distributed across stable forest, stable non-forest and deforestation classes from the tree cover maps from Wagner et al. (2023) to account for potential commission and omission errors in these areas. We aimed to select a minimum of 30 samples per date from 2017 to 2021. The final number for our presence classes were: 331 samples for logging, 569 for fire, and 342 for roads. The sample size per class was higher than the minimum recommendation of 98, 106, 71 samples for logging, fire, and roads, respectively, considering stratified samples and a 1% standard error for overall accuracy calculated following Olofsson et al. (2014) good practices. After the stratified random sampling design was done, we observed 70% of samples occurred over forests (stable or deforested in between 2017 and 2021) and 30% over stable non-forests. The high number of samples in the absence strata (absence of a given disturbance) was used as a strategy to reduce uncertainties associated with omission errors (Olofsson et al., 2020; Olofsson, 2021). The degradation classes can overlap each other, so the same forest can be for example logged and then burned, which is slightly different from conventional land use and cover change (LUCC) analyses.

To create the reference classification of our samples we conducted visual interpretation of high-resolution Planet NICFI imagery (4.7 m spatial resolution) between 2016 and 2022 at the Collect Earth Online platform (Saah et al., 2019). Two images per year were used in the platform dashboard as reference data for the interpreters to answer the survey regarding each sample. The survey was designed following a continuous monitoring assessment approach where each sample was analyzed to determine the year of occurrence of a given disturbance or its absence (Arévalo et al., 2020). Each disturbance was allowed to occur independently from each other, i.e. logging and fire at the same sample. Three interpreters experienced in LUCC and degradation visual interpretation conducted the data collection, where two interpreters collected the initial samples (having >90% agreement between each other), and a third senior interpreter reviewed the results. To ensure high quality on the sampling outcomes, for each sample, the interpreters also assigned a confidence level (low or high). Samples with low confidence were considered as non-reliable to be used for the analysis and were removed from analysis (the final number of 2678 samples already discounted the low confidence samples). We note that using multiple images from the Planet NICFI time series for interpretation is key for the accurate interpretation of these disturbances. Especially for forest fires' burn scars, some samples are difficult to interpret and required the comparison of images across time to make sure the patterns observed were indeed burn scars and not some natural change in vegetation. Also, for fire it is important to zoom out of the sample, because some burn scar patterns are easier to identify when looking at larger contexts. The samples with a given identified disturbance occurring in the year 2016 were removed from analysis, because analyses were done starting from year 2017.

After validation data were collected, we estimated and reported the mean and 90% confidence interval for overall, producer's and user's accuracy, F_1-*score*, as well as for the area estimate of each class considering the validation data as reference and accounting for uncertainties in the maps (Olofsson et al., 2014). This reference dataset was also used to evaluate the relative performance of our method in comparison to existing datasets of forest disturbance: DETER, SIMEX, Global Forest Change (GFC), Tropical Moist Forests (TMF), Global Fire Loss (FireGFL), FireCCI, MCD64, MapBiomas Fire, and GABAM. In order to estimate accuracies using the same reference dataset obtained from the map strata of DL-DEGRAD, we employed the method by Stehman (2014) that was designed for strata being different from the assessed map classes. The calculations were done using the *'mapaccuracy'* R-package (Costa, 2022). For this analysis we filtered areas of non-forest from the compared data products. A full description of these datasets and pre-processing is presented in Supplementary Material S2 and Supplementary Table S1. First, the maps were assessed in terms of location, that is, whether the product found that sample-pixel to be disturbed in any period from 2017 to 2020. Second, they were analyzed in terms of date of occurrence, that is, if the product found the correct period of disturbance from 2017 to 2020. To analyze the date of occurrence, the weighted F1-Score (*WF$_1$-score)* was computed by taking the mean F_1-*score* among the different detected years corrected by the number of pixels found in that year. The F_1-*score* calculated for each year assumes that any detection found outside of that year is incorrect.

2.3.3. Spatial agreement of degradation products

To understand the spatial agreement between products, we also conducted an inter-comparison analysis comparing each pair of products pixel per pixel (Supplementary Table S1). For this analysis, we aggregated detections from 2017 to 2020. For this analysis we did not filter areas of non-forest from the compared data products and used their original detections. Each pair of data products were compared to calculate the recall and Intersection over Union (IoU) metrics. The recall corresponds to the percentage of area mapped by one product to a reference, in this case considering SIMEX and DETER as references. The IoU corresponds to the ratio between the overlap area mapped by the two products and the total area mapped by the two products and was calculated in between all pairs of data products. The goal here was to determine the overlap between data products, and understand which one more closely resembles official Brazilian datasets (DETER and SIMEX), considering them as 'ground truth', to the best extent of spatial resolution and visual interpretation limitations from which they were created.

2.3.4. Degradation area and frequency in Mato Grosso

Finally, the degradation was analyzed across the study area regarding area and frequency of each disturbance. Degradation data were aggregated into the 20 × 20 km tiles before calculating the fraction of degraded forests from 2016 to 2021 normalized by the remaining forest in 2021. To retrieve remaining forest areas, we used the tree cover and deforestation dataset based on Planet NICFI data and DL model (Wagner et al., 2023). The frequency of degradation was analyzed by looking at degraded areas from the year 2017 from our cumulative degradation product, and by tabulating how many times areas were found as degraded afterwards using our frequency of degradation product. Total degraded forest areas and deforestation per year for Mato Grosso were calculated from 2017 to 2021.

3. Results

3.1. Model validation for individual mosaic prediction

The U-Net DL model showed very high overall accuracy (> 98%) and a F_1-*score* of 0.82 on segmenting the disturbances caused by logging, fire, and road construction on an individual mosaic (August 2021) considering the 20% validation data not used for training (Table 2). For logging and fire, the DL model showed recall values higher than precision values ($R = 0.90$ and 0.88, respectively), indicating the ability of the proposed approach for accurately detecting most of the validation samples. However, it also had 20–25% commission errors ($P = 0.75$ and 0.80,

Table 2
Performance of the deep learning (DL) model using Planet NICFI data to map degraded forests on image patches of an individual mosaic (August 2021). The metrics of accuracy were calculated using the 20% validation samples (14,749 patches of 256 × 256 pixels, or 22,123 km^2).

	Precision (P)	Recall (R)	F_1-*Score*	Accuracy (%)
Logging	0.75	0.90	0.82	98.20
Fire	0.80	0.88	0.84	98.42
Roads	0.69	0.61	0.65	99.36

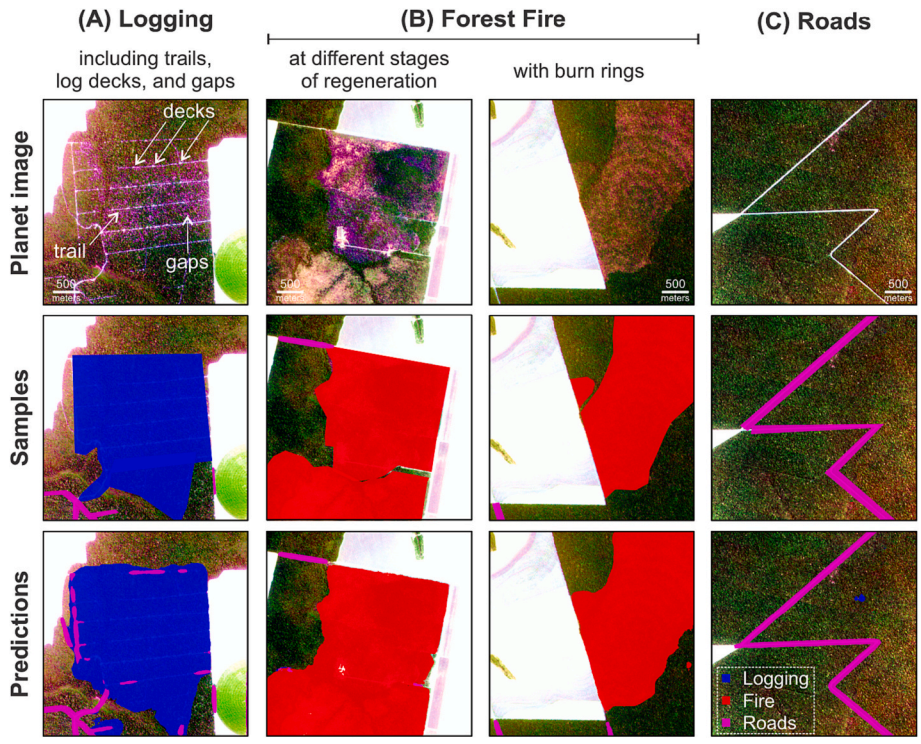

Fig. 3. Examples of degradation by logging (A), forest fire (B) and road construction (C) mapped by the deep learning (DL) model in an individual mosaic. The first row shows Planet NICFI true color composites, while the second row illustrates manually delimited samples over the corresponding areas. The third row indicates the DL model prediction results.

respectively). The road construction detection had an inferior performance (F_1-*score* = 0.65) than that observed for logging (F_1-*score* = 0.82) and fire (F_1-*score* = 0.84).

DL-DEGRAD accurately detected and mapped the boundary of areas degraded by logging around logging trails, decks, and canopy gaps (Fig. 3A). Irregular or small-scale logging, without trails or logging decks, were also detected when canopy gaps were visible in the imagery (Supplementary Fig. S6). The model accurately segmented burned forests with different levels of burn intensity and stages of regenerating vegetation, including areas with burn rings (Fig. 3B). The DL model correctly mapped roads/trails that were found in the middle of the forest, and not only roads neighboring other land covers (Fig. 3C). Wider logging trails were sometimes detected in the roads class (Fig. 3A). However, individual roads were rarely confused as logging.

3.2. Accuracy estimates

Considering the design-based stratified random reference samples (n = 2678 samples), DL-DEGRAD products showed predictions that presented strong agreement with logging identified in reference data for both location (F_1-*score* = 68.9) and correct year of detection (WF_1-*score* = 57.1) (Table 3). SIMEX and DETER also showed strong to moderate agreement with the reference data with logging for both location (F_1-*score* values of 69.3 and 51.3, respectively) and year (WF_1-*score* = 56.4

Table 3
Map agreement between the DL-DEGRAD product (this study) and other available products for the detection of logging and forest fire degradation considering a probability design-based stratified sample design (n = 2678 samples). Overall Accuracy (OA), User's Accuracy (UA), Producer's Accuracy (PA), and F1-score values are shown in percentage, from 0 to 100%. Values in bold were the metrics with the highest performance.

Disturbance and Products	Location of disturbance detected from 2017 to 2020				Correct year of disturbance detected from 2017 to 2020	
	OA%	UA%	PA%	F_1-*score*	OA%	Weighted F_1-*score* (WF_1)
Logging						
DL-DEGRAD Logging	97.9	57.4	**86.2**	68.9	97.4	**57.1**
SIMEX	**98.5**	**80.9**	60.7	**69.3**	**98.2**	56.4
DETER Logging	97.7	61.4	44.3	51.5	97.4	37.7
GFC	82.6	5.6	33.0	9.5	82.2	4.2
TMF	93.9	8.0	11.4	9.4	93.9	4.9
Forest Fire						
DL-DEGRAD Fire	97.6	65.5	**89.5**	75.6	97.3	**69.1**
DETER Fire	**98.5**	**87.0**	75.7	**81.0**	**97.5**	52.7
FireGFL	97.2	74.2	49.1	59.1	96.4	38.0
GFC	91.0	24.5	57.0	34.3	89.9	20.6
FireCCI	89.4	16.8	39.1	23.5	88.6	10.4
MCD64	89.6	15.7	34.3	21.6	88.8	7.5
TMF	94.8	27.5	16.5	20.6	94.5	9.4
GABAM	91.4	13.4	19.7	16.0	90.8	3.2
MapBiomas Fire	88.8	6.5	12.7	8.6	88.4	1.9
Road						
DL-DEGRAD Road	**97.7**	**29.5**	**55.1**	**38.4**	**97.4**	**23.8**

and 37.7, respectively). Both GFC and TMF products showed weak agreement with the reference dataset for samples with identified logging (F_1-*score* = 9.5 and 9.4, respectively). For degradation caused by fire, DL-DEGRAD showed strong agreement with the reference data for both location (F_1-*score* = 75.6) and correct year of detection (WF_1-*score* = 69.1). DETER and FireGFL also showed strong to moderate agreement with the fire reference data for location (F_1-*score* values of 81.0 and 59.1) and moderate for the date (WF_1-*score* values of 52.7 and 38.0). The remaining datasets showed moderate to weak agreement with the fire reference data showing F_1-*scores* ranging from 8.6 to 34.3. The DL-DEGRAD road mapping had moderate agreement for location (F_1-*score* = 38.4) and weak for date (WF_1-*score* = 23.8). Confusion matrices, accuracies and area estimates with confidence intervals are found in Supplementary Materials S3 and Supplementary Tables from S2 to S9.

By inspecting the user and producer's accuracies of products with highest performances, we observed that DL-DEGRAD results for logging and fire showed high producer's accuracy considering only location (PAs of 86.2 and 89.5%, respectively), and moderate user's accuracy (UAs of 57.4 and 65.5%, respectively). This means that most of the degradation was found by the model (omission errors of 14% and 10% for logging and fire, respectively), but additional areas not belonging to the disturbance classes were mapped as disturbance (commission errors of 43 and 34% for logging and fire, respectively). The opposite was found for the other data products, where UA was higher than PA, indicating the products could not reliably detect most disturbances in the reference data, but their detections were generally correct when they did map it. For instance, SIMEX had the highest UA for logging (80.9%) and DETER the highest UA for fire (87%). On the other hand, the two datasets showed lower PAs of 60.7% and 75.7%, respectively, indicating they omitted from 24 to 39% of the degradation events.

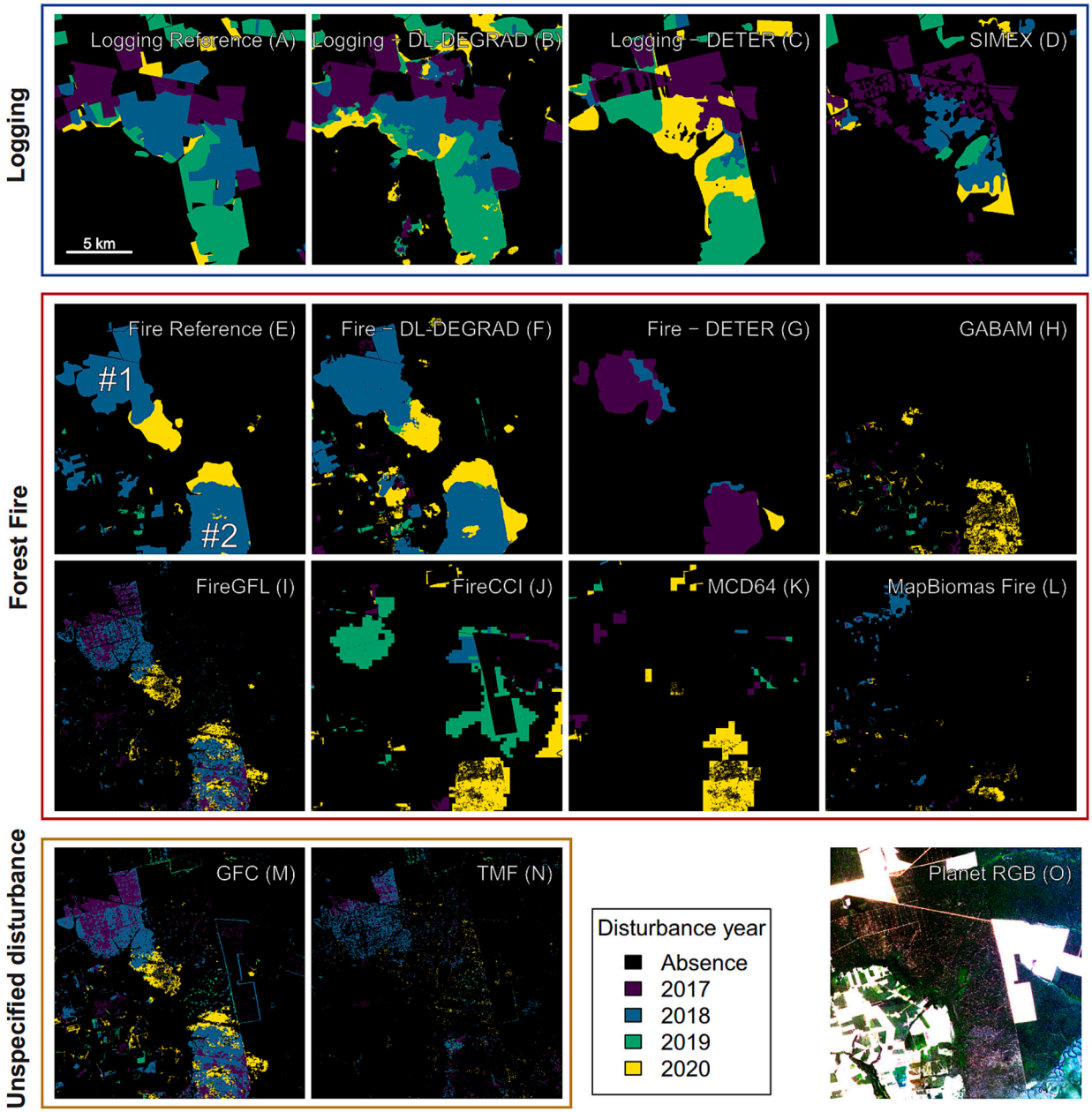

Fig. 4. Examples of cumulative forest degradation maps from the DL-DEGRAD and available products from 2017 to 2020 for a site located at 54°14′W; 12°7′S. (A-D) Logging mapped by the independent test dataset, DL-DEGRAD Logging, DETER Logging, and SIMEX, respectively. (*E*-L) Forest fire mapped by the independent test dataset, DL-DEGRAD Fire, DETER Fire, GABAM, FireGFL, FireCCI, MCD64, and MapBiomas Fire, respectively. (M-N) Unspecified Forest disturbances mapped by the GFC and TMF. (O) Planet NICFI true color composite from June 2020.

To understand better these commission and omission errors, we inspected them one by one and found that in the case of logging as mapped by SIMEX, 59% of samples with omission were small-scale logging activities without road infrastructure (with bare soil showing on the trails), 19% were logged forests with very clear patterns of road infrastructure and likely large enough to be observed in Landsat imagery, 13% were simple human interpretation errors when drawing the vectors, and 9% occurred in areas with clear logging patterns but overlap with burn scars. In the case of the omissions of fire mapped in DETER dataset, 56% of omissions were large-scale fires being omitted (e.g. > 500 m width), errors of geolocation (displaced detections to the patterns observed in the imagery), burn scars not being mapped at logged forests (the same but inverse issue as SIMEX), or an erroneous attribution to deforestation alert or to DETER's 'degradation' mosaic class which may mix both logging and fire, 23% related to small-scale or less severe burn scars that vanish quickly from the imagery (disappear in 6–12 months), and 21% related to random errors due to the sample being close to the edge of the burn scar or the forest edge, and the polygon was off by up to 100 m (few Landsat pixels).

In agreement with the results of Table 3, we found a strong agreement between the independent test dataset and our DL-DEGRAD product when visually inspecting the degradation by logging mapped with the different products (Fig. 4A-D). Results were also consistent with the detections of SIMEX (based on official Mato Grosso state logging concessions data) and DETER (official national degradation data from INPE). The GFC and TMF (Fig. 4L and M) showed scattered detections in correct locations of logged forests, depicting logging trails and decks. However, the detections by these two products did not encompass the whole boundary of the logged forests. GFC showed many detections in locations unrelated to degradation by logging, such as in the bottom-left corner of the area (Fig. 4). Those areas are recently burned and deforested areas. The degradation by fire in the example revealed strong agreement between our DL-DEGRAD product and the reference dataset, and some disagreement with the other products, especially regarding the disturbance year (Fig. 4E-K). For example, the area #1 (Fig. 4E) which burned in 2018 (in blue) was mapped as burned in 2018 by our product and GFC. It was mapped as burned in 2017 by DETER and in 2019 by FireCCI. MapBiomas Fire and MCD64 did not fully detect that event. Furthermore, for the burned area #2 (Fig. 4E) that burned in 2018 and 2020 (in blue and yellow), DL-DEGRAD mapped the first fire occurrence in 2018, while GFC and DETER also mapped parts of the area as being burned in 2018 and 2017, respectively. The remaining products did not detect the first fire, and only mapped that area as burned in 2020 when a second fire happened. GFC showed a good match for fire, but also detected many pixels that did not correspond to fire disturbance. More examples to highlight the performance of the model can be observed in the Supplementary Material S2, including examples of a mix of logging and fire occurrences at different dates at site B (Supplementary Fig. S7), large-scale fires occurring at different dates at site C (Supplementary Fig. S8), and logging occurring at different dates at site D (Supplementary Fig. S9).

3.3. Spatial agreement of degradation products

DL-DEGRAD mapped 77.89% and 64.76% of the total logged forests present in SIMEX and DETER datasets, respectively (Table 4). On the other hand, GFC and TMF mapped <20% of the total logging present in SIMEX and DETER. Regarding forest fire, DL-DEGRAD mapped 72.59% of all forest fire observed in DETER, while the next highest recalls or overlaps were observed for FireCCI (44.13%) and GFC (41.07%) datasets. When looking at the intersection-over-union metrics between all products (Tables 5 and 6), meaning the intersecting area mapped by two products divided by the total area mapped by both, DL-DEGRAD also showed the highest overlap with DETER (IoU = 20.89%) and SIMEX (IoU = 27.87%) for logging degradation. The other data products showed a very low overlap with SIMEX or DETER (IoU close to 5%). For fire degradation, DL-DEGRAD showed the highest agreement with DETER (IoU = 33.47%). Among the other tested products, the FireGFL product also showed high overlap with DETER (IoU = 28.66%).

3.4. Degradation extent in Mato Grosso rainforests

According to the DL-DEGRAD product and probability design-based area estimates, 42,216.1 km^2 of forests have been degraded by logging

Table 4
Percentage of SIMEX and DETER detections of logging and forest fire mapped by data products (Recall metric) considering any detection from 2017 to 2020. Values with highest overlap/recall are highlighted in bold.

Product	Logging		Fire
	Overlap SIMEX (%)	Overlap DETER Logging (%)	Overlap DETER Fire (%)
DL-DEGRAD Logging	**77.89**	**64.76**	–
SIMEX	–	48.22	–
DETER Logging	45.16	–	–
TMF	9.30	9.75	13.31
GFC	15.48	19.01	41.07
DL-DEGRAD Fire	–	–	**72.59**
FireCCI	–	–	44.13
MCD64	–	–	37.80
FireGFL	–	–	36.26
GABAM	–	–	20.58
MapBiomas Fire	–	–	18.02

Table 5
Logging and roads degradation products' intercomparison. Values represent the agreement between products measured by the pixel-by-pixel Intersection over Union (IoU) metrics, considering any detection from 2017 to 2020.

	DL-DEGRAD Logging	DL-DEGRAD Roads	SIMEX	DETER Logging	TMF	GFC
DL-DEGRAD Logging	–	2.48	27.87	20.89	3.73	5.05
DL-DEGRAD Roads	2.48	–	1.70	1.48	1.47	3.47
SIMEX	27.87	1.70	–	30.41	4.82	4.55
DETER Logging	20.89	1.48	30.41	–	4.89	5.36
TMF	3.73	1.47	4.82	4.89	–	9.29
GFC	5.05	3.47	4.55	5.36	9.29	–

Table 6
Fire degradation products' intercomparison. Values represent the agreement between products measured by the pixel-by-pixel Intersection over Union (IoU) metrics, considering any detection from 2017 to 2020.

	DL-DEGRAD Fire	DETER Fire	GABAM	MCD64	FireCCI	MapBiomas Fire	TMF	GFC	FireGFL
DL-DEGRAD Fire	–	33.47	9.56	12.14	15.25	7.80	8.93	24.21	21.94
DETER Fire	33.47	–	9.23	10.63	13.25	5.95	9.38	20.81	28.66
GABAM	9.56	9.23	–	29.23	36.94	42.60	0.66	15.22	8.70
MCD64	12.14	10.63	29.23	–	43.40	32.64	1.77	12.12	8.06
FireCCI	15.25	13.25	36.94	43.40	–	38.45	2.38	15.39	9.87
MapBiomas Fire	7.80	5.95	42.60	32.64	38.45	–	0.66	10.97	5.04
TMF	8.93	9.38	0.66	1.77	2.38	0.66	–	9.29	9.75
GFC	24.21	20.81	15.22	12.12	15.39	10.97	9.29	–	45.38
FireGFL	21.94	28.66	8.70	8.06	9.87	5.04	9.75	45.38	–

Table 7
Degradation area estimates from DL-DEGRAD and deforestation area estimates from Wagner et al., 2023 in the Mato Grosso Rainforests from 2017 to 2021 according to design-based estimates conducted in this study. Values in parentheses represent the 90% Confidence Interval around the mean for the stratified sample estimator.

	DL-DEGRAD (this study)			Wagner et al., 2023
	Logging (km^2)	Forest Fire (km^2)	Roads (km^2)	Deforestation (km^2)
2017	1332.9 (±623)	2335.6 (±453)	2083.3 (±713)	2534.3 (±853)
2018	3404.2 (±884)	6709.6 (±944)	532.6 (±385)	7486.3 (±1479)
2019	4068.7 (±655)	2223.2 (±449)	1640.5 (±736)	4508.2 (±932)
2020	4159.8 (±973)	9134.6 (±1204)	941.7 (±539)	6594.3 (±1472)
2021	4969.7 (±1084)	3877.7 (±863)	1250.4 (±715)	5536.8 (±1169)
Total	17,935.4	24,280.7	6448.5	26,659.8

and fire over the Amazon biome portion of the Mato Grosso state from 2017 to 2021, corresponding to an average degradation rate of 8443 $km^2\ yr^{-1}$ (Table 7). Furthermore, both deforestation and degradation increased from 2017 to 2021 in the study area. The relative contribution of each degradation type to the total degradation area was 58% to fire (4856 $km^2\ yr^{-1}$ on average) and 42% to logging (3587 $km^2\ yr^{-1}$). The absolute road area estimates were not combined with logging and fire due to an overestimate of roads' width by the model, however the estimates show that road construction is ongoing in the region of Mato Grosso. The sum of annual degradation by logging and fire exceeded deforestation rates in all years. On average, the combined annual degradation by logging and fire was 58% higher (8443 $km^2\ yr^{-1}$) than the annual deforestation (5332 $km^2\ yr^{-1}$) (Fig. 5; Supplementary Table S11). In 2020, the combined degradation rate of logging and fire reached a record high of 13,294 km^2, or two times the deforested area for that year, which was 6594 km^2. While logging rates were high in 2020, degradation due to fire was the major responsible for the higher rates in that year.

Forest degradation by logging was widespread across the study area with some areas reaching >40% degradation at west of the Xingu Park (Fig. 5A). Areas inside and at the east of Xingu Park showed relatively less impacts from logging. On the other hand, degradation by fire was more concentrated in the southwest of the Mato Grosso state, as well as inside and west of the Xingu Park, where our model detected fire-induced degradation reaching >60% of forests (Fig. 5B). Inside the Xingu Park, we observed very large patches of burned forests close to the major rivers, reaching up to 250 km^2 for a single fire event. We found widespread degradation from narrow roads or trails across the study area, where almost every forest area has some trail access that is not immediately noted in color composites when visual interpreting, even at the 4.77 m resolution. The center of the Mato Grosso region showed the highest concentrations of roads inside the forests (>25%), mainly associated with land use activities. The concentrations of roads decreased towards the north of the state (Fig. 5C). The three indigenous territories of Aripuanã Park, Apiaká do Pontal e Isolados, and Xingu Park showed the least degraded forests of the state and the most remaining forests in 2021 (Fig. 5D). Their boundaries were easily visualized in Fig. 5C, as indicated by blue colors (close to zero % roads).

The distribution of the temporal frequency of detections of logging and fire degradation showed different patterns (Fig. 6). Logging had on average 50% more detections on the same pixel (4.27 detections) than fire (2.85 detections). The frequency of logging detections gradually decreased from one detection (23% with one detection) up to ten detections, but never reached <5%. Meanwhile, the frequency of fire detections increased from one to two detections (24 to 29%) and then decreased to <1% for eight or more detections.

From the areas found as degraded by logging and fire in our maps in between 2017 and 2021, 24% of them had been further subject to deforestation by the end of 2021. An estimated 301,960 km^2 of standing forests remained in the Amazonian biome of Mato Grosso in 2021 (Supplementary Table S9), accounting for 59.5% of the total area. Of these remaining forests, 14% or 42,216 km^2 were identified as degraded during the analysis period from 2017 to 2021.

4. Discussion

4.1. The novelty of the DL-DEGRAD approach

We successfully developed and validated the first tropical forest degradation map based on 4.77-m resolution Planet NICFI satellite data with detection and attribution of logging, fire, and road construction in the Brazilian Amazon forests in the state of Mato Grosso. Overall, the DL-DEGRAD approach showed 97% accuracy and 68.9%, 75.6% and 38.4% *F_1-scores* for logging, fire, and road construction degradation mapping according to the probability design-based accuracies estimates. Compared to existing approaches and previous results, we summarize the novelty of our methodology in three contributions: (1) Our methodology is designed to automatically map areas impacted by forest degradation (forest remaining forest by losing carbon and change of structure) with close to human level accuracy, similarly as regional official datasets as DETER and SIMEX, and not only mapping pixels with complete clearings or cover change (Hansen et al., 2013); (2) The U-Net model developed in our study is different from earlier deep-learning models for detecting tree cover loss and deforestation (Wagner et al., 2023), by being trained to map degradation from combined tree loss and textural variations in high resolution imagery. In addition to improved resolution, the accuracy of detecting degradation is significantly better than results based on Landsat imagery (Vancutsem et al., 2021); (3) Our

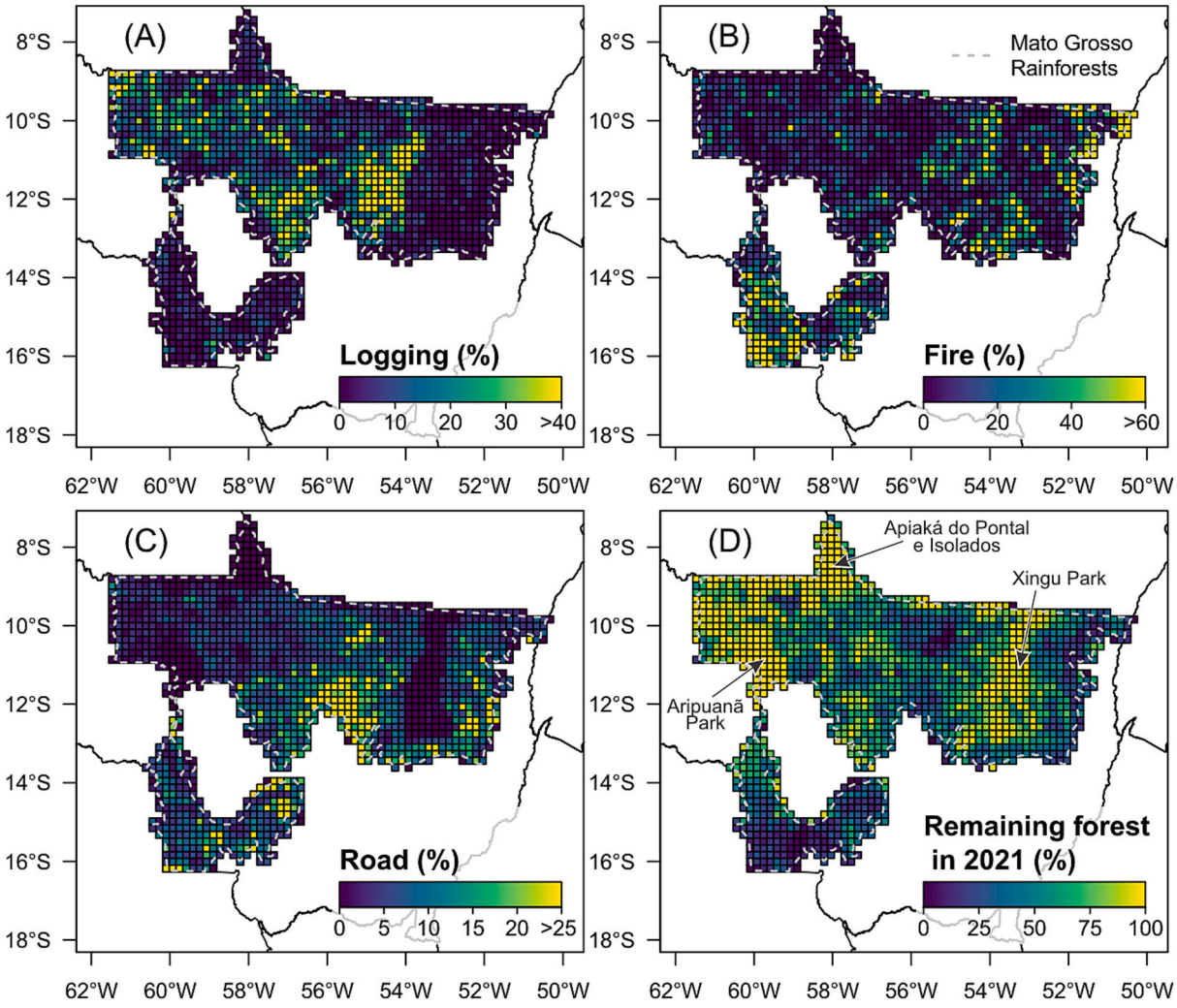

Fig. 5. Percentage of degraded forests from 2016 to 2021 shown by the DL-DEGRAD product for the disturbances caused by (A) logging, (B) fire, and (C) road construction. The panel (D) represents the percentage of remaining intact forests in the year 2021. Each cell corresponds to a 20 × 20 km tile. Values were truncated at their 95th percentile to improve visualization.

approach provides attributions to several events of forest degradation caused by logging, forest fire, and roads. The attributions are important for assessing the carbon loss and emission for various scientific and greenhouse gas (GHG) inventory and reporting (Pearson et al., 2017). Forest degradation affects large areas of the Amazon and has important effects on the global carbon cycle (Aragão et al., 2014).

The model showed high agreement on determining the exact year of degradation, with some variability in the year-to-year user's and producer's accuracy but with no clear trend. This means that even though we trained the model mostly using only the mosaic of one date (August 2021), it was able to learn the spatial features associated with degradation and reproduce that across time and space. This is an important feature of our model, because one of the main purposes of having such a model is reducing the manual effort to produce maps at different locations and over multiple years, therefore overcoming limitations of noise in the PlanetScope data and ultimately being able to achieve mapping at large scale. We expect this ability to generalize to other locations and dates may be attributed to multiple components of the training dataset. First, there is a lot of reflectance variability in the Planet NICFI imagery even when using data from a single month: image mosaics are composed of aggregated images from hundreds of small satellites collecting data at different angles which creates lots of noise and acquisition artifacts. Second, the spatial variability of the training data includes most of the forest covers existing in the Southern Amazon, from open to dense forests and some short stature savanna-type forests, which contributes for its adaptation to different locations and dates. We note however, for heavily seasonal forests, the model and methodology might need to be adapted in future studies. During the period of analysis (December 2015 to December 2021), some improvements in technical specifications of the CubeSats (e.g., radiometric resolution) were implemented over time. Although not evaluated in our work, the effects of these improvements on the results are probably small because of the use of composite products selecting the highest quality pixels in a given month or biannual period.

We advanced forest degradation mapping by developing a workflow that combines AI analysis with remote sensing data of both high spatial and temporal resolution. First, the applied U-Net DL model learned the spatial patterns associated with the different disturbances in one time period. Then, it was able to predict degradation with high accuracy to different areas within Mato Grosso for image composites covering different time periods. Historically, mapping logging with satellite imagery has focused on detecting trails and log decks with high soil fractions using spectral unmixing techniques (Souza et al., 2005). However, this kind of mapping does not return area estimates close to the real extent of logged forests, which correspond to the bounding box around trees that have been logged. By mapping the area of logged forests, that is, the boundaries around trails, log decks, and treefall gaps (whenever visible), our method and dataset produce area estimates close to the

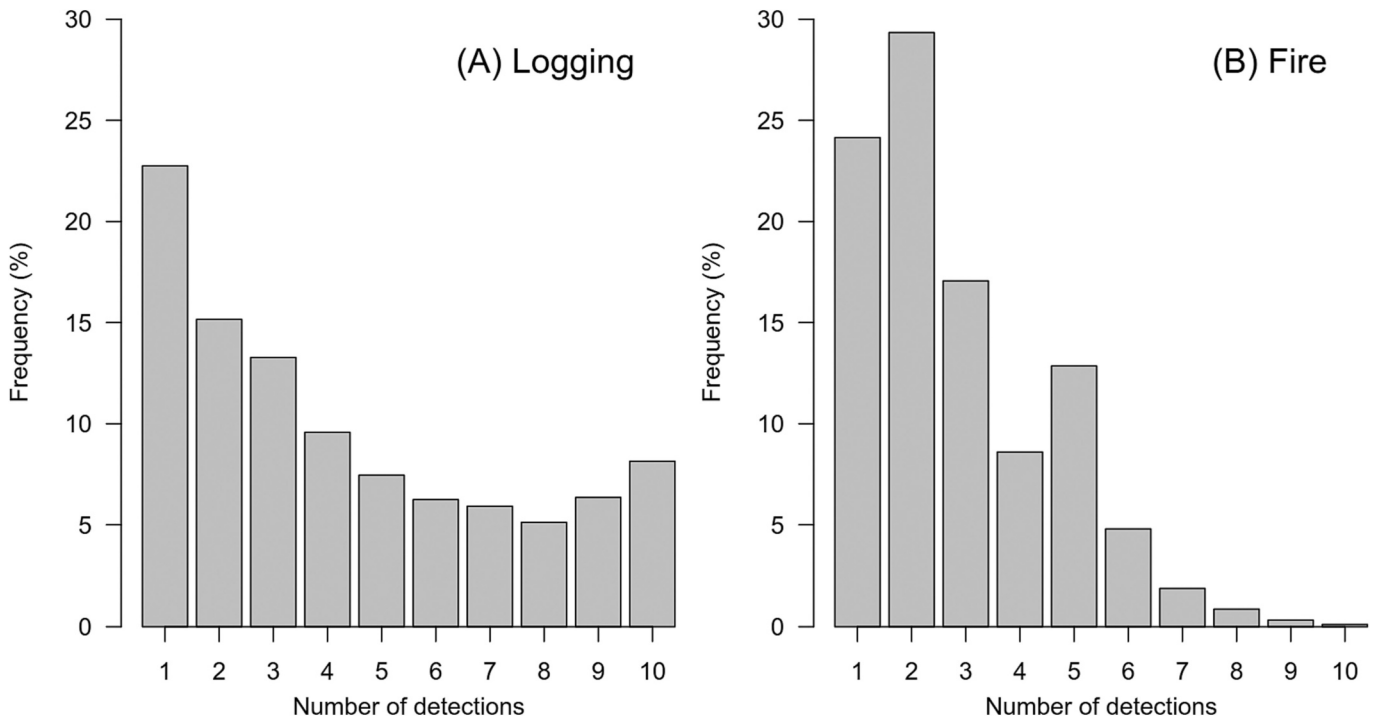

Fig. 6. Per-pixel temporal frequency of degradation detection by DL-DEGRAD, initially mapped in 2017 by (A) Logging, and (B) Fire disturbances.

extent of degraded forests. This is supported by the high overlap between DL-DEGRAD with SIMEX data, which considers logging permits for areas of forest management (Silgueiro et al., 2021). Small-scale logging was also captured by DL-DEGRAD, in which the occurrence of roads was not the main feature for disturbance detection (example shown in Supplementary Fig. S6). Second, the model also leveraged the high temporal resolution of PlanetScope imagery to map forest degradation every six months, that is, before the regeneration can cover the tracks of disturbance. This contributed to show that logging disturbances lingered for a longer time in the imagery than the footprints from fire disturbances. On average, our frequency data indicated that logging patterns persisted in the imagery for 2.13 years, while fire patterns persisted in the imagery for 1.42 years. This means that at least annual datasets are required to fully capture forest degradation effects, especially those caused by fire, which is easily achievable by the PlanetScope data.

4.2. Comparison of degradation products

Among the degradation products compared in the analysis, DL-DEGRAD logging and fire maps showed one of the highest F1-scores according to the design-based stratified random sampling approach used here, in relation to the correct location as well as the correct timing of degradation. The results brought by DL-DEGRAD showed similar performance to those from regional datasets of DETER and SIMEX based on visual interpretation of satellite data and manual delineation of degradation. While considering limitations of data comparison, the difference between DL-DEGRAD and SIMEX for mapping logged forests was <1% of F1-Score; and for forest fire, DETER had 5% higher F1-Score on identifying the location, but 16% less F1-Score on identifying the correct year of degradation than the DL-DEGRAD. Moreover, a similar outcome was observed when we compared the pixel-by-pixel agreement between data products, where DL-DEGRAD showed the highest agreement with the visual-interpreted regional datasets DETER and SIMEX when compared to the other automatic datasets. This reinforces that it is not a matter of the data used for the evaluation or their spatial resolution, but that the methodology is in fact mapping forest degradation more consistently and with human-level accuracy when compared to other automatic methods. One difference, however, is that DL-DEGRAD mapped two to three times more areas of degradation than DETER and SIMEX, thereby finding areas that were not previously mapped. We note however, as shown in the results, part of these mapped areas can be attributed to commission errors from DL-DEGRAD, but also to omission errors from SIMEX and DETER. Area estimates should be done using the design-based approach, which accommodates errors in the maps. We expect our dataset to complement these initiatives to obtain more accurate maps of forest degradation, as well as making them more efficient and consistent than visual inspection. While performing visual interpretation and manual data collection for such large areas may take months of work by trained analysts, through our model framework we can map the entire Mato Grosso rainforest area (>500,000 km^2) from new Planet NICFI monthly image composites in less than one day.

An in-depth look into the omission errors in SIMEX for Logging (39.3%) and DETER for Fire (24.3%) reveals that 60 and 44% of these errors of these two datasets, respectively, are likely not avoidable when using Landsat data because they consist of (i) small-scale patterns which only appeared in one Planet NICFI bi-annual mosaic and then disappeared in the next mosaic, that is, vegetation quickly recovered in a matter of six to twelve months; and (ii) logging areas without well-built road infrastructure; or (iii) image resolution-related issues, such as omission of fire at the borders of burn scars. On the other hand, some errors can be avoided, such as logging not being identified if the area was also burned (also the inverse), DETER geolocation errors showing detections displaced from 80 to 200 m of the actual degradation, and omitted large-scale forest fires (e.g. >500 m of width) which could be clearly seen in the Landsat imagery but were not mapped by DETER. By deducing the potentially avoidable errors (40 and 66% of logging and fire), we estimate the Landsat data would allow the observation up to a theoretical maximum of 84.3 and 84% of all logging and fire in the reference dataset. This reveals a limitation to what Landsat data may offer for visual interpretation of degradation in the Mato Grosso region, of which shows large logging infrastructure and large forest fire events. Thus, if the dynamics of logging in other regions involve less development of infrastructure (e.g., illegal logging), or fires are smaller in size,

the rate of detection using Landsat data will likely decrease. Nevertheless, although having higher commission errors than SIMEX and DETER – a rate that can be reduced in further developments of the model, our DL approach using Planet NICFI allows to observe much more of these small-scale logging activities with low omission errors (10%).

The DL-DEGRAD approach offers improved mapping abilities for logging degradation that are not matched by any other automatic data product, and that reduces the minimum area mapped by visual-interpreted datasets (DETER and SIMEX) based on 30-m satellite data. Moreover, the DL-DEGRAD product showed higher sensitivity in detecting forest fires than the compared automatic burned area products. Besides DL-DEGRAD, the FireGFL dataset also showed good agreement for fire degradation mapping (*F1-Score* of 59.1). We find that the FireGFL is an important refinement over the GFC product because it mainly retrieves forest fires reducing other sources of disturbance (Tyukavina et al., 2022). The remaining automatic burned area maps had low map agreements (F_1*-score* lower than 34%). This low map agreement was especially observed regarding time of detection, which highly varied between burned area products, indicating the high uncertainty to map burned forests using available datasets. We expect that our methodology can contribute to surpass previous limitations of understory fire mapping sensitivities (Morton et al., 2011; Dupuis et al., 2020; Gao et al., 2020). By visual examining the Planet NICFI imagery, we identified that burned area products usually detected burned forests when the fire severity was high and barely any vegetation was left, corresponding to brown to black colors in the NICFI true color composites. Therefore, underestimating understory fires obfuscated by the forest canopy (Morton et al., 2011). Meanwhile, our DL-DEGRAD product was trained to detect different levels of fire severity and post-fire regeneration. Therefore, even if there is a temporal mismatch between fire occurrence and image acquisition, we can detect it afterwards. Even with coarser spatial resolution data, the MCD64 showed similar performance to FireCCI (difference of 2% in *F1-Score*) and better agreement with the reference data than other products such as the GABAM and MapBiomas Fire. This corroborated a previous finding that MCD64 had better performance than Landsat-based satellite estimates of fire disturbance (Pessôa et al., 2020).

4.3. Limitations

The differences in spatial and temporal resolution between the compared data products bring some potential limitations in the data analysis. Also, the accuracy metrics of the compared datasets represent the accuracy of the resampled (down-sampled) datasets and according to the degradation definitions utilized in this study. This type of comparison is complex and has intrinsic limitations as discussed in previous studies (Tyukavina et al., 2017; Pessôa et al., 2020). This is the reason why an effort was made here to provide independent reference data as well as to compare products on a per-pixel basis. We note that there is also subjectivity in manual vectorization of degradation of which there is not a simple solution. The boundary of the degraded areas is usually not sharp and well defined such as a forest/non-forest boundary, and its interpretation can vary according to the interpreter – as also highlighted some issues in complementary products such as SIMEX and DETER. However, after training the DL model to perform the mapping, it can provide a more consistent and reliable approach to map the boundaries of degraded forests based on the data, thus following the spectral/textural features of which humans may lack visual acuity to identify boundaries or manual dexterity to accurately draw them. However, the good agreement presented between our automated approach and manually delineated products (DETER and SIMEX) highlight the method is able to reproduce what other analysts also identified as degradation in these official datasets. A thorough assessment of degradation intensity and how much of it leads to a detection is yet to be assessed in future studies. For logging degradation, this means acquiring and integrating data of carbon losses in logging concessions at state and national level, however for degradation due to fire, ground data is way more limited. Analysis of airborne lidar data may help to address these gaps in future studies.

The spatial extent of mapped roads covers a larger area than the actual disturbed area, resulting in the overestimation of the road-covered areas, as shown by the low user's accuracy in the probability design-based validation (29.5%). At the current state, the road maps should not be used for direct area estimates. It can be useful though as a relative indicator of road coverage and increase over time. This estimate will be improved for next versions of this data product by reducing the width of the road training samples to match more closely the width of the interpreted roads and trails. The overestimation does not affect its potential use for monitoring where roads are being opened, and how they can contribute to the spread of degradation, of which the road maps can do a nice job (Supplementary Fig. S10). The spatial extent of areas degraded by logging and fire mapped by the DL-DEGRAD approach is higher than other methods that mostly track complete canopy clearings, but a strong spatial agreement is observed with degraded forests mapped by SIMEX and DETER datasets (Silgueiro et al., 2021; De Almeida et al., 2022). These estimates differ from other datasets, such as GFC and TMF, which detect only pixels with tree loss pixels (change from forest to bare soil), explaining the much higher detected area by our method. Due to the inability to look under the canopy and to the quick gap recovery dynamics of vegetation, we expect that the exact degraded area estimate at local scales should be very hard to achieve using optical data of any spatial resolution in the future. This area could be potentially retrieved at local scales using ALS data looking at the top of the canopy and understory. Overall, at regional scales, we expect that DL-DEGRAD has potential to capture most of the degraded forests, but some small-scale disturbances where forest can quickly recover may still be underestimated. The ability of the dataset to observe repeated degradation in the same area is still to be assessed in future research, when more data collection on repeated events is collected.

During the DL training, we discovered and dealt with a few issues arising from artifacts of Planet NICFI imagery as well as from the different environments of the Amazon forests. The level of accuracy obtained was only possible because the U-Net model inherently learns the contextual information in the imagery, which minimizes issues of reflectance variability and visual artifacts present in PlanetScope data, caused by the nature of their acquisition system - a constellation of hundreds of small satellites (Pandey et al., 2021). Some notable artifacts from Planet NICFI data include areas where apparent dust clouds were found nearby cities in Mato Grosso likely due to radiometric correction (Supplementary Fig. S1); illumination artifacts in the edges of forests where saturated brighter signals were found (Supplementary Fig. S11); and brightness effects created by the mosaicking in locations of severe cloud influence (Supplementary Fig. S3-S5). The brightness effects were dealt with by including samples of those locations in the training dataset. To minimize the cloud issues, we developed our own cloud mapping model to mask out remaining clouds in the Planet NICFI product. Other issues related to Amazonian environments that caused the model to produce false positives and commission errors were large flowering trees being confused with logging (likely because their round shape could be confused with a logging deck, as well as having low NIR values), and narrow rivers being confused with roads. These reported issues were minimized in predictions by adding examples of these occurrences as samples of absence of degradation during model training.

Alternative sources of high-resolution data to the Planet NICFI include the Sentinel-1 and Sentinel-2 satellite sensors operating at a similar spatial resolution (10-m) (Zhang et al., 2021; Reiche et al., 2021). In this context, some recent studies have shown the potential of Sentinel-2 to map small-scale disturbances (< 1 ha) associated with shifting agriculture and logging roads (Zhang et al., 2021). The potential of Sentinel-1 to map forest disturbances from logging roads and large canopy gaps with exposed soil has also been demonstrated (Reiche et al., 2021). However, it is yet to be investigated whether Sentinel data brings

enough contextual information for the CNN-based method to map degradation without apparent tree loss.

4.4. Impacts

Our study represents the first large-scale attempt to use a DL model to map tropical forests degraded by logging, fire and road construction based on high-resolution Planet NICFI satellite data. This is the first step towards developing large-scale operational monitoring of degradation, required to understand the extent of tropical forests degradation and its impacts to carbon, as well as achieve goals of REDD+ at jurisdictional levels (Mitchell et al., 2017). By stratifying forest degradation between different drivers, it is possible to obtain more accurate emission estimates using specific emission factors for each type of disturbance (Rappaport et al., 2018). This is the type of information that the Mato Grosso government is currently using from the SIMEX (logging) and INPE's DETER (logging and fire) products. Both products are based on visual interpretation and manual vectorization of maps, but can now be produced in an automatic and timely manner through our approach. In the context of REDD+, policy and decision making, where pixel counting may not be the preferred approach, the maps generated by the DL-DEGRAD approach can be used as a starting point for a sample-based approach to estimating the areas of land cover and change as shown in this paper (Olofsson et al., 2014; Global Forest Observations Initiative, 2020).

The implementation of near real-time forest monitoring from bi-annual to monthly, or even weekly, time-steps should be possible with further developments. Planet NICFI provides unprecedented open high-resolution data (4.77-m) at bi-annual (Dec 2015 to Jun 2020) to monthly frequency from September 2020 to recent days, which allows for the continuous monitoring of forest degradation in the future, given the continuity of the program. For this first experiment, we accumulated the monthly predictions into six-month composites to increase confidence in results and to secure the same time-intervals for the entire time-series. However, by improving our models with more training data, as well as testing alternative DL architectures, we expect to increase confidence in monthly predictions. This could be especially useful to help authorities performing ground operations with greater agility over national parks under threat or over selected areas targeting the frontiers of deforestation and degradation. Such a near-real time approach will also be useful to monitor individual REDD+ carbon projects, where forest protection and carbon sequestration are of major concern.

Our findings show Mato Grosso rainforests have been going through widespread and very-high rates of degradation due to logging and fire corresponding to 8443 km^2 yr^{-1} from 2017 to 2021. Around 24% of these degraded areas have already been deforested by 2021, depicting the pathway of which degradation leads to deforestation. The remaining forests in 2021 account for 301,960 km^2, of which 14% were assessed as degraded in between 2017 and 2021. Overall, these degradation estimates exceed by a factor of two to three those from official datasets from DETER/INPE. Part of this degradation is in fact legalized though state logging concessions program (Silgueiro et al., 2021). However, that does not change the fact that these forests dynamics are being widely changed without much thought to what this will mean for the future of the Amazon forests and potential impacts to the climate. Meanwhile, recent studies point out that logged forests are a net source of carbon to the atmosphere (Mills et al., 2023). The year 2020 alone was responsible for 31.5% of the five-year degradation, that is, 13,294 km^2 of the total 42,215 km^2 area of degradation mapped in the region, and to twice the deforestation rate of that year, with a major contribution from fires with 9134 km^2 of burned forests. Indigenous territories within Mato Grosso had significantly lower levels of degradation compared to other areas. Protecting these territories from spilling deforestation and degradation are of utmost importance as already highlighted in previous studies (de Oliveira et al., 2022).

Overall, our study reveals a dire situation for southern Amazonian rainforests in the edge of 'arc of deforestation', of which degradation has been rampant in these last few years and leading to further deforestation activities. The technology necessary to accurately put degradation on the map is available through the presented methodology. Knowing where degraded forests are located can be important to assess carbon dynamics following disturbance, in terms of both carbon losses but also gains as expected if these forests are allowed to regenerate (Heinrich et al., 2023). It is essential that next studies stratify between planned and unplanned deforestation, logging and fire activities, because each process may have different carbon dynamics and mechanisms which policymakers and environmental agencies can pursue to optimize nature-based solutions to climate change. If Brazil wants to effectively tackle REDD+, hampering the further spread of degradation is imperative and must be considered together with the zero-deforestation pledge until 2030.

5. Conclusions

Tropical forest degradation can now be mapped at a cost-efficient manner with an unprecedented level of detail in spatial and temporal scales using a trained U-Net deep learning model applied to Planet NICFI data. Moreover, it is possible to provide attributions to the causes of degradation (logging, forest fire, and road construction), which can contribute to ensuring the degradation classes are well represented in the samples being used for area estimates on REDD+ monitoring. We also show that at least annual temporal resolution is necessary to reliably map degraded forests. The performance of our automated approach was found to be consistent with degradation products generated from visual interpretation of 30-m satellite data and substantial manual editing (e.g., DETER and SIMEX). However, the NICFI data allows mapping degradation with additional detail which is likely not possible with Landsat. Our new DL-DEGRAD approach shows that the tropical forests of Mato Grosso are being degraded by logging and fire at the rate of 8443 km^2 yr^{-1}. Of the remaining forests in 2021 (301,960 km^2), at least 14% are currently degraded. In the period of analysis, 2020 showed the largest area of degradation (13,294 km^2), exceeding deforestation twofold. In the future, the model will be evaluated and improved to extend the mapping of forest degradation across the entire pan-tropical forests.

Author contributions

R.D., F.W. and S·S. contributed to research conceptualization; R.D. and F.W. developed the codes to run the models; R.D., D.B., M.P., and F. O. collected the training and validation samples; R.D. conducted the formal analysis with inputs from F.W., L.B.S. and S.S; R.D. wrote the first draft of the manuscript; All authors reviewed and edited the manuscript and provided critical feedback on the paper's discussion and improvement; S.S. supervised the research. All authors have read and agreed to the published version of the manuscript.

Funding

The authors are grateful to the Grantham and High Tide Foundations for their generous gift to UCLA and grants to CTrees for bringing new science and technology to solve environmental problems. This work was partially conducted at the Jet Propulsion Laboratory, California Institute of Technology under a contract (80NM0018F0590) the National Aeronautics and Space Administration (NASA). R.D. was partially supported by the São Paulo Research Foundation (FAPESP) grant 2019/21662-8. D.B. was supported by the Brazilian National Council for Scientific and Technological Development (CNPq). P.C.B. and M.P. were supported by the University of Manchester through SEED (School of Environment Education and Development) New Horizons Research & Scholarship Stimulation Fund. L.O.A. was supported by the FAPESP grants: 2020/15230-5 and 2020/08916, FAPEAM grant 01.02.016301.000289/2021-

33 and the National Council for Scientific and Technological Development (CNPq), Brazil, productivity grant 314473/2020-3. R.F. is supported by the research grant DeReEco (34306) from Villum Fonden.

Declaration of Competing Interest

The authors declare no conflict of interest. The funders had no role in the design of the study; in the collection, analyses, or interpretation of data; in the writing of the manuscript, or in the decision to publish the results.

Data availability

The Planet NICFI data were accessed through Level-2 partnership with the NICFI program.

Acknowledgements

We thank NICFI initiative, and the Level-2 access granted to R.D., which was imperative to conduct this large-scale study. We thank SERVIR and FAO for the Collect Earth Online (CEO) platform which allowed the collection of reference data for the design-based accuracy and area assessment in this study. We thank four reviewers and editor Marie Weiss for insightful comments that helped improve this manuscript.

Appendix A. Supplementary data

S1 – Cloud cover mapping, Supplementary Material S2 – Data products for comparison, Supplementary Material S3 – Model results, detailed accuracy and area results. Supplementary Fig. S1 to S11. Supplementary Table S1 to S11.

References

Alencar, A.A.C., Arruda, V.L.S., da Silva, W.V., Conciani, D.E., Costa, D.P., Crusco, N., Duverger, S.G., Ferreira, N.C., Franca-Rocha, W., Hasenack, H., Martenexen, L.F.M., Piontekowski, V.J., Ribeiro, N.V., Rosa, E.R., Rosa, M.R., dos Santos, S.M.B., Shimbo, J.Z., Vélez-Martin, E., 2022. Long-term landsat-based monthly burned area dataset for the brazilian biomes using deep learning. Remote Sens. 14 (11), 2510. https://doi.org/10.3390/rs14112510.

Allaire, J., Chollet, F., 2016. keras: R Interface to 'Keras' (2.14). https://github.com/rstudio/keras.

De Almeida, C.A., Câmara, G., Motta, M., Gomes, A.R., Amaral, S., 2022. METODOLOGIA UTILIZADA NOS SISTEMAS PRODES E DETER - 2 a EDIÇÃO (ATUALIZADA). http://urlib.net/8JMKD3MGP3W34T/47GAF6S.

Andela, N., Morton, D.C., Schroeder, W., Chen, Y., Brando, P.M., Randerson, J.T., 2022. Tracking and classifying Amazon fire events in near real time. Sci. Adv. 8 (30), 1–12. https://doi.org/10.1126/sciadv.abd2713.

Aquino, C., Mitchard, E.T.A., Mcnicol, I.M., Carstairs, H., Burt, A., Luz, B., Vilca, P., Mayta, S., Disney, M., 2022. Detecting tropical Forest degradation using optical satellite data : an experiment in Peru show texture at 3 M gives best results. Preprints February, 1–21. https://doi.org/10.20944/preprints202202.0141.v1.

Aragão, L.E.O.C., Poulter, B., Barlow, J.B., Anderson, L.O., Malhi, Y., Saatchi, S., Phillips, O.L., Gloor, E., 2014. Environmental change and the carbon balance of amazonian forests. Biol. Rev. 89 (4), 913–931. https://doi.org/10.1111/brv.12088.

Aragão, L.E.O.C., Anderson, L.O., Fonseca, M.G., Rosan, T.M., Vedovato, L.B., Wagner, F. H., Silva, C.V.J., Silva Junior, C.H.L., Arai, E., Aguiar, A.P., Barlow, J., Berenguer, E., Deeter, M.N., Domingues, L.G., Gatti, L., Gloor, M., Malhi, Y., Marengo, J.A., Miller, J.B., Saatchi, S., 2018. 21st century drought-related fires counteract the decline of Amazon deforestation carbon emissions. Nat. Commun. 9 (1), 1–12. https://doi.org/10.1038/s41467-017-02771-y.

Arévalo, P., Olofsson, P., Woodcock, C.E., 2020. Continuous monitoring of land change activities and post-disturbance dynamics from landsat time series: a test methodology for REDD+ reporting. Remote Sens. Environ. 238 (January 2019), 111051 https://doi.org/10.1016/j.rse.2019.01.013.

Asner, G.P., Keller, M., Silva, J.N.M., 2004. Spatial and temporal dynamics of forest canopy gaps following selective logging in the eastern Amazon. Glob. Chang. Biol. 10 (5), 765–783. https://doi.org/10.1111/j.1529-8817.2003.00756.x.

Asner, G.P., Knapp, D.E., Broadbent, E.N., Oliveira, P.J.C., Keller, M., Silva, J.N., 2005. Selective logging in the brazilian Amazon. Science 310 (5747), 480–482. https://doi.org/10.1126/science.1118051.

Barni, P.E., Rego, A.C.M., Silva, F.C.F., Lopes, R.A.S., Xaud, H.A.M., Xaud, M.R., Barbosa, R.I., Fearnside, P.M., 2021. Logging Amazon forest increased the severity and spread of fires during the 2015–2016 El Niño. Forest Ecol. Manage. 500 https://doi.org/10.1016/j.foreco.2021.119652.

Bomfim, B., Pinagé, E.R., Emmert, F., Kueppers, L.M., 2022. Improving sustainable tropical forest management with voluntary carbon markets. Plant Soil 479 (1–2), 53–60. https://doi.org/10.1007/s11104-021-05249-5.

Botelho, J., Costa, S.C.P., Ribeiro, J.G., Souza, C.M., 2022. Mapping roads in the brazilian Amazon with artificial intelligence and sentinel, 2.

Brandt, M., Tucker, C.J., Kariryaa, A., Rasmussen, K., Abel, C., Small, J., Chave, J., Rasmussen, L.V., Hiernaux, P., Diouf, A.A., Kergoat, L., Mertz, O., Igel, C., Gieseke, F., Schöning, J., Li, S., Melocik, K., Meyer, J., Sinno, S., Fensholt, R., 2020. An unexpectedly large count of trees in the west african Sahara and Sahel. Nature 587 (7832), 78–82. https://doi.org/10.1038/s41586-020-2824-5.

Brasil, 2021. LEI no 14.119, DE 13 DE JANEIRO DE 2021: Política nacional de pagamento por Serviços ambientais.

Bullock, E.L., Woodcock, C.E., 2021. Carbon loss and removal due to forest disturbance and regeneration in the Amazon. Sci. Total Environ. 764, 142839 https://doi.org/10.1016/j.scitotenv.2020.142839.

Bullock, E.L., Woodcock, C.E., Souza, C., Olofsson, P., 2020. Satellite-based estimates reveal widespread forest degradation in the Amazon. Glob. Chang. Biol. 26 (5), 2956–2969. https://doi.org/10.1111/gcb.15029.

Chollet, F., 2015. Keras. https://keras.io.

Chollet, F., Kalinowski, T., Allaire, J.J., 2022. Deep learning with R, 2nd ed. Manning.

Chuvieco, E., Lizundia-Loiola, J., Lucrecia Pettinari, M., Ramo, R., Padilla, M., Tansey, K., Mouillot, F., Laurent, P., Storm, T., Heil, A., Plummer, S., 2018. Generation and analysis of a new global burned area product based on MODIS 250 m reflectance bands and thermal anomalies. Earth Syst. Sci. Data 10 (4), 2015–2031. https://doi.org/10.5194/essd-10-2015-2018.

Costa, H., 2022. Map accuracy: unbiased thematic map accuracy and area. R Pack. Vers. (1), 1. https://CRAN.R-project.org/package=mapaccuracy.

Cunningham, D., Cunningham, P., Fagan, M.E., 2019. Identifying biases in global tree cover products: a case study in Costa Rica. Forests 10 (10). https://doi.org/10.3390/f10100853.

Dalagnol, R., Phillips, O.L., Gloor, E., Galvão, L.S., Wagner, F.H., Locks, C.J., Aragão, L.E. O.C., 2019. Quantifying canopy tree loss and gap recovery in tropical forests under low-intensity logging using VHR satellite imagery and airborne LiDAR. Remote Sens. 11 (7), 817. https://doi.org/10.3390/rs11070817.

Dalagnol, R., Wagner, F.H., Emilio, T., Streher, A.S., Galvão, L.S., Ometto, J.P.H.B., Aragão, L.E.O.C., 2022. Canopy palm cover across the Brazilian Amazon forests mapped with airborne LiDAR data and deep learning. Remote Sens. Ecol. Conserv. 1–14 https://doi.org/10.1002/rse2.264.

de Oliveira, G., Mataveli, G.A.V., Dos Santos, C.A.C., He, L., Hellenkamp, S.E., Funatsu, B.M., Stark, S.C., Shimabukuro, Y.E., 2022. Protecting Amazonia should focus on protecting indigenous, traditional peoples and their territories. Forests 13 (1), 2017–2020. https://doi.org/10.3390/f13010016.

Dice, L.R., 1945. Measures of the amount of ecologic association between species. Ecology 26 (3), 297–302. https://doi.org/10.2307/1932409.

Dupuis, C., Lejeune, P., Michez, A., Fayolle, A., 2020. How can remote sensing help monitor tropical moist forest degradation?-a systematic review. Remote Sens. 12 (7) https://doi.org/10.3390/rs12071087.

Falbel, D., Allaire, J., RStudio, Tang, Eddelbuettel, D., Golding, N., Kalinowski, T., Inc, Google, 2022. tensorflow: R Interface to "TensorFlow" (R package 2.9.0).

Ferrante, L., Fearnside, P.M., 2020. The Amazon ' s road to deforestation smoke pollution ' s impacts in Amazonia funding quandary. Sci. Lett. 369 (6504), 634–635.

Gao, Y., Skutsch, M., Paneque-Gálvez, J., Ghilardi, A., 2020. Remote sensing of forest degradation: a review. Environ. Res. Lett. 15 (10), 2000–2010. https://doi.org/10.1088/1748-9326/abaad7.

Giglio, L., Boschetti, L., Roy, D.P., Humber, M.L., Justice, C.O., 2018. The collection 6 MODIS burned area mapping algorithm and product. Remote Sens. Environ. 217 (March), 72–85. https://doi.org/10.1016/j.rse.2018.08.005.

Global Forest Observations Initiative, 2020. Integrating remote-sensing and ground-based observations for estimation of emissions and removals of greenhouse gases in forests, June, 300.

Gourlet-Fleury, S., Mortier, F., Fayolle, A., Baya, F., Ouédraogo, D., Bénédet, F., Picard, N., 2013. Tropical forest recovery from logging: a 24 year silvicultural experiment from Central Africa. Phil. Trans. R. Soc. B 368 (1625). https://doi.org/10.1098/rstb.2012.0302.

Hansen, M.C., Potapov, P.V., Moore, R., Hancher, M., Turubanova, S.A., Tyukavina, A., Thau, D., Stehman, S.V., Goetz, S.J., Loveland, T.R., Kommareddy, A., Egorov, A., Chini, L., Justice, C.O., Townshend, J.R.G., 2013. High-resolution global maps of 21st-century forest cover change. Science 342 (6160), 850–853. https://doi.org/10.1126/science.1244693.

Heinrich, V.H.A., Vancutsem, C., Dalagnol, R., Rosan, T.M., Fawcett, D., Silva-Junior, C. H.L., Cassol, H.L.G., Achard, F., Jucker, T., Silva, C.A., House, J., Sitch, S., Hales, T. C., Aragão, L.E.O.C., 2023. The carbon sink of secondary and degraded humid tropical forests. Nature 615 (7952), 436–442. https://doi.org/10.1038/s41586-022-05679-w.

IPCC, 2003. In: Penman, J., Gytarsky, M., Hiraishi, T., Krug, T., Kruger, D., Pipatti, R., Buendia, L., Miwa, K., Ngara, T., Tanabe, K. (Eds.), Definitions and Methodological Options to Inventory Emissions from Direct Human-induced Degradation of Forests and Devegatation of Other Vegetation Types. Miura: Ins, pp. 3–32.

Joseph, S., Herold, M., Sunderlin, W.D., Verchot, L.V., 2013. REDD+ readiness: early insights on monitoring, reporting and verification systems of project developers. Environ. Res. Lett. 8 (3) https://doi.org/10.1088/1748-9326/8/3/034038.

Kattenborn, T., Leitloff, J., Schiefer, F., Hinz, S., 2021. Review on convolutional neural networks (CNN) in vegetation remote sensing. ISPRS J. Photogramm. Remote Sens. 173 (January), 24–49. https://doi.org/10.1016/j.isprsjprs.2020.12.010.

Kingma, D.P., Ba, J.L., 2015. Adam: A method for stochastic optimization. In: 3rd International Conference on Learning Representations, ICLR 2015 - Conference Track Proceedings, pp. 1–15.
Kinnebrew, E., Ochoa-Brito, J.I., French, M., Mills-Novoa, M., Shoffner, E., Siegel, K., 2022. Biases and limitations of global Forest change and author-generated land cover maps in detecting deforestation in the Amazon. PLoS ONE 17 (7 July), 1–23. https://doi.org/10.1371/journal.pone.0268970.
Lapola, D.M., Pinho, P., Barlow, J., Aragão, L.E.O.C., Berenguer, E., Carmenta, R., Liddy, H.M., Seixas, H., Silva, C.V.J., Silva-Junior, C.H.L., Alencar, A.A.C., Anderson, L.O., Armenteras, D., Brovkin, V., Calders, K., Chambers, J., Chini, L., Costa, M.H., Faria, B.L., Walker, W.S., 2023. The drivers and impacts of Amazon forest degradation. Science 379 (6630). https://doi.org/10.1126/science.abp8622.
Lecun, Y., Bengio, Y., Hinton, G., 2015. Deep learning. Nature 521 (7553), 436–444. https://doi.org/10.1038/nature14539.
Lobo Torres, D., Queiroz Feitosa, R., Nigri Happ, P., Elena Cué La Rosa, L., Marcato Junior, J., Martins, J., Olã Bressan, P., Gonçalves, W.N., Liesenberg, V., 2020. Applying fully convolutional architectures for semantic segmentation of a single tree species in urban environment on high resolution UAV optical imagery. Sensors 20 (2), 563. https://doi.org/10.3390/s20020563.
Long, T., Zhang, Z., He, G., Jiao, W., Tang, C., Wu, B., Zhang, X., Wang, G., Yin, R., 2019. 30m resolution global annual burned area mapping based on landsat images and Google earth engine. Remote Sens. 11 (5), 1–30. https://doi.org/10.3390/rs11050489.
Matricardi, E.A.T., Skole, D.L., Pedlowski, M.A., Chomentowski, W., Fernandes, L.C., 2010. Assessment of tropical forest degradation by selective logging and fire using landsat imagery. Remote Sens. Environ. 114 (5), 1117–1129. https://doi.org/10.1016/j.rse.2010.01.001.
Matricardi, E.A.T., Skole, D.L., Costa, O.B., Pedlowski, M.A., Samek, J.H., Miguel, E.P., 2020. Long-term forest degradation surpasses deforestation in the brazilian Amazon. Science 369 (6509), 1378–1382. https://doi.org/10.1126/SCIENCE.ABB3021.
Melendy, L., Hagen, S.C., Sullivan, F.B., Pearson, T.R.H., Walker, S.M., Ellis, P., Sambodo, A.K., Roswintiarti, O., Hanson, M.A., Klassen, A.W., Palace, M.W., Braswell, B.H., Delgado, G.M., 2018. Automated method for measuring the extent of selective logging damage with airborne LiDAR data. ISPRS J. Photogramm. Remote Sens. 139, 228–240. https://doi.org/10.1016/j.isprsjprs.2018.02.022.
Mills, M.B., Malhi, Y., Ewers, R.M., Kho, L.K., Teh, Y.A., Both, S., Burslem, D.F.R.P., Majalap, N., Nilus, R., Huaraca Huasco, W., Cruz, R., Pillco, M.M., Turner, E.C., Reynolds, G., Riutta, T., 2023. Tropical forests post-logging are a persistent net carbon source to the atmosphere. Proc. Natl. Acad. Sci. 120 (3), 2017. https://doi.org/10.1073/pnas.2214462120.
Mitchell, A.L., Rosenqvist, A., Mora, B., 2017. Current remote sensing approaches to monitoring forest degradation in support of countries measurement, reporting and verification (MRV) systems for REDD+. Carbon Balance Manage. 12 (1) https://doi.org/10.1186/s13021-017-0078-9.
Morton, D.C., DeFries, R.S., Nagol, J., Souza, C.M., Kasischke, E.S., Hurtt, G.C., Dubayah, R., 2011. Mapping canopy damage from understory fires in Amazon forests using annual time series of landsat and MODIS data. Remote Sens. Environ. 115 (7), 1706–1720. https://doi.org/10.1016/j.rse.2011.03.002.
Mouselimis, L., 2022. PlanetNICFI: Processing of the "Planet NICFI" Satellite Imagery Using R (R Package v1.0.4)..
Nascimento, E.S., da Silva, S.S., Bordignon, L., de Melo, A.W.F., Brandão, A., Souza, C.M., Silva Junior, C.H.L., 2021. Roads in the southwestern amazon, state of acre, between 2007 and 2019. Land 10 (2), 1–12. https://doi.org/10.3390/land10020106.
NICFI, 2021. NICFI Data Program https://www.nicfi.no/.
Nicfi, 2023. In: Planet Basemaps For NICFI Data Program: Addendum To Basemaps Product Specification, December, pp. 1–6.
Olofsson, P., 2021. Updates to good practices for estimating area and assessing accuracy of land cover and land cover change products. Int. Geosci. Remote Sens. Symp. (IGARSS) 1982–1985. https://doi.org/10.1109/IGARSS47720.2021.9554475.
Olofsson, P., Arévalo, P., Espejo, A.B., Green, C., Lindquist, E., McRoberts, R.E., Sanz, M.J., 2020. Mitigating the effects of omission errors on area and area change estimates. Remote Sens. Environ. 236 (January 2019), 111492 https://doi.org/10.1016/j.rse.2019.111492.
Olofsson, P., Foody, G.M., Herold, M., Stehman, S.V., Woodcock, C.E., Wulder, M.A., 2014. Good practices for estimating area and assessing accuracy of land change. Remote Sens. Environ. 148, 42–57. https://doi.org/10.1016/j.rse.2014.02.015.
Pandey, A.K.P., Kington, J., Curdoglo, M., 2021. Addendum to planet basemaps. product specifications. Nicfi Basemaps 02.
Pearson, T.R., Brown, S., Murray, L., Sidman, G., 2017. Greenhouse gas emissions from tropical forest degradation: an underestimated source. Carbon Balance Management 12 (1), 3. https://doi.org/10.1186/s13021-017-0072-2.
Pereira, R., Zweede, J., Asner, G.P., Keller, M., 2002. Forest canopy damage and recovery in reduced-impact and conventional selective logging in eastern Para, Brazil. Forest Ecol. Manage. 168 (1–3), 77–89. https://doi.org/10.1016/S0378-1127(01)00732-0.
Pessôa, A.C.M., Anderson, L.O., Carvalho, N.S., Campanharo, W.A., Junior, C.H.L.S., Rosan, T.M., Reis, J.B.C., Pereira, F.R.S., Assis, M., Jacon, A.D., Ometto, J.P., Shimabukuro, Y.E., Silva, C.V.J., Pontes-Lopes, A., Morello, T.F., Aragão, L.E.O.C., 2020. Intercomparison of burned area products and its implication for carbon emission estimations in the Amazon. Remote Sens. 12 (23), 3864. https://doi.org/10.3390/rs12233864.
Pinagé, E.R., Keller, M., Peck, C.P., Longo, M., Duffy, P., Csillik, O., 2023. Effects of forest degradation classification on the uncertainty of aboveground carbon estimates in the Amazon. Carbon Balance Manage. 18 (1), 2. https://doi.org/10.1186/s13021-023-00221-5.
Qin, Y., Xiao, X., Wigneron, J.P., Ciais, P., Brandt, M., Fan, L., Li, X., Crowell, S., Wu, X., Doughty, R., Zhang, Y., Liu, F., Sitch, S., Moore, B., 2021. Carbon loss from forest degradation exceeds that from deforestation in the brazilian Amazon. Nat. Clim. Chang. 11 (5), 442–448. https://doi.org/10.1038/s41558-021-01026-5.
Rappaport, D.I., Morton, D.C., Longo, M., Keller, M., Dubayah, R., Dos-Santos, M.N., 2018. Quantifying long-term changes in carbon stocks and forest structure from Amazon forest degradation. Environ. Res. Lett. 13 (6), 2000–2010. https://doi.org/10.1088/1748-9326/aac331.
Reiche, J., Mullissa, A., Slagter, B., Gou, Y., Tsendbazar, N.E., Odongo-Braun, C., Vollrath, A., Weisse, M.J., Stolle, F., Pickens, A., Donchyts, G., Clinton, N., Gorelick, N., Herold, M., 2021. Forest disturbance alerts for the Congo Basin using Sentinel-1. Environ. Res. Lett. 16 (2) https://doi.org/10.1088/1748-9326/abd0a8.
Ronneberger, O., Fischer, P., Brox, T., 2015. U-net: convolutional networks for biomedical image segmentation. In: Lecture Notes in Computer Science (Including Subseries Lecture Notes in Artificial Intelligence and Lecture Notes in Bioinformatics), 9351, pp. 234–241. https://doi.org/10.1007/978-3-319-24574-4_28.
Saah, D., Johnson, G., Ashmall, B., Tondapu, G., Tenneson, K., Patterson, M., Poortinga, A., Markert, K., Quyen, N.H., San Aung, K., Schlichting, L., Matin, M., Uddin, K., Aryal, R.R., Dilger, J., Lee Ellenburg, W., Flores-Anderson, A.I., Wiell, D., Lindquist, E., Chishtie, F., 2019. Collect earth: an online tool for systematic reference data collection in land cover and use applications. Environ. Model. Softw. 118 (March), 166–171. https://doi.org/10.1016/j.envsoft.2019.05.004.
Shimabukuro, Y.E., Arai, E., Duarte, V., Jorge, A., dos Santos, E.G., Gasparini, K.A.C., Dutra, A.C., 2019. Monitoring deforestation and forest degradation using multi-temporal fraction images derived from landsat sensor data in the brazilian Amazon. Int. J. Remote Sens. 40 (14), 5475–5496. https://doi.org/10.1080/01431161.2019.1579943.
Shimabukuro, Y.E., Miettinen, J., Beuchle, R., Grecchi, R.C., Simonetti, D., Achard, F., 2015. Estimating burned area in Mato Grosso, Brazil, using an object-based classification method on a systematic sample of medium resolution satellite images. IEEE J. Sel. Top. Appl. Earth Obs. Remote Sens. 8 (9), 4502–4508. https://doi.org/10.1109/JSTARS.2015.2464097.
Silgueiro, V., Cardoso, B., Valdiones, A.P., Batista, L., 2021. Mapping illegality in logging in Mato Grosso in 2020 (Issue October). https://www.icv.org.br/biblioteca/.
Silva Junior, C.H.L., Carvalho, N.S., Pessôa, A.C.M., Reis, J.B.C., Pontes-Lopes, A., Doblas, J., Heinrich, V., Campanharo, W., Alencar, A., Silva, C., Lapola, D.M., Armenteras, D., Matricardi, E.A.T., Berenguer, E., Cassol, H., Numata, I., House, J., Ferreira, J., Barlow, J., Aragão, L.E.O.C., 2021. Amazonian forest degradation must be incorporated into the COP26 agenda. Nat. Geosci. 14 (9), 634–635. https://doi.org/10.1038/s41561-021-00823-z.
Silva, C.V.J., Aragão, L.E.O.C., Barlow, J., Espirito-Santo, F., Young, P.J., Anderson, L.O., Berenguer, E., Brasil, I., Brown, I.F., Castro, B., Farias, R., Ferreira, J., França, F., Graça, P.M.L.A., Kirsten, L., Lopes, A.P., Salimon, C., Scaranello, M.A., Seixas, M., Xaud, H.A.M., 2018. Drought-induced amazonian wildfires instigate a decadal-scale disruption of forest carbon dynamics. Phil. Trans. R. Soc. B 373 (1760). https://doi.org/10.1098/rstb.2018.0043.
Silva, C.H.L., Aragão, L.E.O.C., Anderson, L.O., Fonseca, M.G., Shimabukuro, Y.E., Vancutsem, C., Achard, F., Beuchle, R., Numata, I., Silva, C.A., Maeda, E.E., Longo, M., Saatchi, S.S., 2020. Persistent collapse of biomass in amazonian forest edges following deforestation leads to unaccounted carbon losses. Sci. Adv. 6 (40), 1–10. https://doi.org/10.1126/sciadv.aaz8360.
Silveira, M.V.F., Silva-Junior, C.H.L., Anderson, L.O., Aragão, L.E.O.C., 2022. Amazon fires in the 21st century: the year of 2020 in evidence. Glob. Ecol. Biogeogr. 31 (10), 2026–2040. https://doi.org/10.1111/geb.13577.
Souza, C.M., Roberts, D.A., Cochrane, M.A., 2005. Combining spectral and spatial information to map canopy damage from selective logging and forest fires. Remote Sens. Environ. 98 (2–3), 329–343. https://doi.org/10.1016/j.rse.2005.07.013.
Souza, C.M., Siqueira, J.V., Sales, M.H., Fonseca, A.V., Ribeiro, J.G., Numata, I., Cochrane, M.A., Barber, C.P., Roberts, D.A., Barlow, J., 2013. Ten-year landsat classification of deforestation and forest degradation in the brazilian amazon. Remote Sens. 5 (11), 5493–5513. https://doi.org/10.3390/rs5115493.
Stehman, S.V., 2014. Estimating area and map accuracy for stratified random sampling when the strata are different from the map classes. International Journal of Remote Sensing 35 (13), 4923–4939. https://doi.org/10.1080/01431161.2014.930207.
Streck, C., 2021. REDD+ and leakage: debunking myths and promoting integrated solutions. Clim. Pol. 21 (6), 843–852. https://doi.org/10.1080/14693062.2021.1920363.
Tyukavina, A., Hansen, M.C., Potapov, P.V., Stehman, S.V., Smith-Rodriguez, K., Okpa, C., Aguilar, R., 2017. Types and rates of forest disturbance in brazilian legal Amazon, 2000–2013. Sci. Adv. 3 (4), 1–16. https://doi.org/10.1126/sciadv.1601047.
Tyukavina, A., Potapov, P., Hansen, M.C., Pickens, A.H., Stehman, S.V., Turubanova, S., Parker, D., Zalles, V., Lima, A., Kommareddy, I., Song, X.-P., Wang, L., Harris, N., 2022. Global trends of Forest loss due to fire from 2001 to 2019. Front. Remote Sens. 3 (March), 1–20. https://doi.org/10.3389/frsen.2022.825190.
Uhl, C., Kauffman, J.B., 1990. Deforestation, fire susceptibility, and potential tree responses to fire in the eastern Amazon. Ecology 71 (2), 437–449. https://doi.org/10.2307/1940299.
Vancutsem, C., Achard, F., Pekel, J.F., Vieilledent, G., Carboni, S., Simonetti, D., Gallego, J., Aragão, L.E.O.C., Nasi, R., 2021. Long-term (1990–2019) monitoring of forest cover changes in the humid tropics. Sci. Adv. 7 (10), 1–22. https://doi.org/10.1126/sciadv.abe1603.
Wagner, F.H., Sanchez, A., Tarabalka, Y., Lotte, R.G., Ferreira, M.P., Aidar, M.P.M., Gloor, E., Phillips, O.L., Aragão, L.E.O.C., 2019. Using the U-net convolutional network to map forest types and disturbance in the Atlantic rainforest with very high resolution images. Remote Sens. Ecol. Conserv. 5 (4), 360–375. https://doi.org/10.1002/rse2.111.

Wagner, F.H., Dalagnol, R., Silva-Junior, C.H.L., Carter, G., Ritz, A.L., Hirye, M.C.M., Ometto, J.P.H.B., Saatchi, S., 2023. Mapping Tropical Forest Cover and Deforestation with Planet NICFI Satellite Images and Deep Learning in Mato Grosso State (Brazil) from 2015 to 2021. Remote Sensing 15 (2), 521. https://doi.org/10.3390/rs15020521.

Wagner, F.H., Dalagnol, R., Tagle Casapia, X., Streher, A.S., Phillips, O.L., Gloor, E., Aragão, L.E.O.C., 2020. Regional mapping and spatial distribution analysis of canopy palms in an Amazon Forest using deep learning and VHR images. Remote Sens. 12 (14), 2225. https://doi.org/10.3390/rs12142225.

Zhang, Y., Ling, F., Wang, X., Foody, G.M., Boyd, D.S., Li, X., Du, Y., Atkinson, P.M., 2021. Tracking small-scale tropical forest disturbances: fusing the landsat and Sentinel-2 data record. Remote Sens. Environ. 261 (April), 112470 https://doi.org/10.1016/j.rse.2021.112470.